QUEZIA PAINS DUTRA

MORPHOPHYSIOLOGICAL IMPACTS ON *Luffa cylindrica* (L.) M. ROEM. AS AFFECTED BY PACLOBUTRAZOL AND CO_2-ENRICHED ATMOSPHERE

Thesis submitted to the Plant Physiology Graduate Program of the Federal University the Viçosa compliance with the requirements for the degree of Doctor Scientiae

Advisor: Wagner Campos Otoni

Co-advisor: Tatiane Dulcineia Silva

VIÇOSA - MINAS GERAIS

2024

QUEZIA PAINS DUTRA

MORPHOPHYSIOLOGICAL IMPACTS ON *Luffa cylindrica* (L.) M. ROEM. AS AFFECTED BY PACLOBUTRAZOL AND CO_2-ENRICHED ATMOSPHERE

Thesis submitted to the Plant Physiology Graduate Program of the Federal University the Viçosa compliance with the requirements for the degree of Doctor Scientiae.

APPROVED: 19 February 2024.

Assent:

Documento assinado digitalmente
gov.br
QUEZIA PAINS DUTRA
Data: 24/07/2024 07:47:25-0300
Verifique em https://validar.iti.gov.br

Quezia Pains Dutra

Author

Documento assinado digitalmente
gov.br
WAGNER CAMPOS OTONI
Data: 21/07/2024 18:16:31-0300
Verifique em https://validar.iti.gov.br

Wagner Campos Otoni

Advisor

Ficha catalográfica elaborada pela Biblioteca Central da Universidade Federal de Viçosa - Campus Viçosa

T
D978m
2024

Dutra, Quezia Pains, 1994-
Morphophysiological impacts on *Luffa cylindrica L.* M. Roem. as affected by paclobutrazol and co2-enriched atmosphere / Quezia Pains Dutra. – viçosa, MG, 2024.
1 tese eletrônica (83 f.): il.

Texto em inglês.
Orientador: Wagner Campos Otoni.
Tese (doutorado) - Universidade Federal de Viçosa, Departamento de Biologia Vegetal, 2024.
Inclui bibliografia.
DOI: https://doi.org/10.47328/ufvbbt.2024.336
Modo de acesso: World Wide Web.

1. Bucha (Planta) - Anatomia - Efeito dos fungicidas. 2. Enzimas. 3. Expressão gênica. 4. Triazol. I. Otoni, Wagner Campos, 1962-. II. Universidade Federal de Viçosa. Departamento de Biologia Vegetal. Programa de Pós-Graduação em Fisiologia Vegetal. III. Título.

CDD 22. ed. 583.63

Bibliotecário(a) responsável: Alice Regina Pinto Pires CRB-6/2523

ACKNOWLEDGEMENTS

Primeiramente, gostaria de agradecer a Deus, pois sem minha fé n'Ele jamais estaria finalizando este doutorado.

Aos meus pais e minhas irmãs por todo ensinamento, incentivo e me ensinar diversos valores como: humildade, respeito e amor. Sem vocês não conseguiria chegar até aqui. Obrigada por tudo!

Aos amigos da família, André e Grisna, que desde a minha graduação sempre estiveram presentes, dando suportes espiritual e financeiro. Lembro-me quando vocês me deram um ventilador quando fui para Alegre fazer graduação. Me marcou muito esse dia!

Ao meu namorado/melhor amigo João Pedro, por todo apoio e incentivo durante toda essa jornada. Obrigada por tudo! Amo você!

À minha co-orientadora Tatiane, não tenho palavras para descrever o quanto sou grata por tudo que você fez por mim. Obrigada por nunca ter desistido de mim e sempre acreditando na minha capacidade como pesquisadora! Voce é gigante mulher!!

Ao meu orientador Wagner Otoni, por todos os ensinamentos e puxões de orelha, por todo suporte em todas as etapas do doutorado. Você sempre será minha inspiração e exemplo de ser humano incrível. O senhor tem um espaço enorme em meu coração e levarei para sempre comigo. Que Deus retribua tudo que o senhor fez/ faz por mim!!!

Aos meus colegas, Michelle Maylla, Elisandra, Dhilermano e Angélica por todo suporte e amizade ao longo desses anos. Voces são incriveis!!

Aos amigos do LCT, Michelle, Jéssica, Gustavo, Lázara, Lana, Pedro, Emerson, Tia Terezinha, Lili e demais colegas, obrigada por todo apoio, das risadas, dos ensinamentos. Nunca se esqueçam do valor de vocês!

Aos meus amigos do Crossfit, em especial Ângela, que nesta etapa final me acolheu de coração. Obrigada por tudo!

À Unidade de Crescimento de Plantas e ao Laboratório de Anatomia Vegetal, por todo suporte para análises de metabolismo e anatomia.

Aos professores do Departamento de Biologia Vegetal, pelas disciplinas oferecidas, que contribuíram de forma valiosa para o meu aprendizado e aos meus colegas da pós-graduação, por todo companheirismo e pela boa convivência.

À Universidade Federal de Viçosa (UFV), principalmente ao Programa de Pós-Graduação em Fisiologia Vegetal, pelo apoio e por fornecer todas as condições necessárias durante o

desenvolvimento da minha pesquisa. Sou também grata à Coordenação de Aperfeiçoamento de Pessoal de Nível Superior – Brasil (CAPES) – Código de Financiamento 001 pela bolsa de estudo concedida e à Fundação de Amparo à Pesquisa do Estado de Minas Gerais [FAPEMIG; APQ-00772-19 e RED-00053-16 - Rede Mineira em Fisiologia de Plantas sob Condições de (Rede Mineira Estresse em Plantas)] e ao Conselho Nacional de Desenvolvimento Científico e Tecnológico (CNPq; Processo 313901/2018-0**;** Processo: 406455/2022-8/Instituto Nacional de Ciência e Tecnologia em Fisiologia de Plantas em Condições de Estresse (INCT Fisiologia do Estresse), pelo suporte financeiro.

Agradeço a todos que direta ou indiretamente contribuíram para a realização deste trabalho, sem vocês eu não teria conseguido. Muito obrigada!

Dedico essa tese ao meu querido pai

ABSTRACT

DUTRA, Quezia Pains, D.Sc., Federal University Viçosa, Febraury, 2024. **Morphophysiological impacts on *Luffa cylindrica* (L.) M. Roem. as affected by Paclobutrazol and CO_2-enriched atmosphere**. Advisor: Wagner Campos Otoni. Co-Advisor: Tatiane Dulcineia Silva.

The plant life cycle involves various strategies to resume growth and development by sensing internal and environmental cues. The environment significantly influences plant metabolism, affecting the production of primary and secondary metabolites. High concentrations of atmospheric CO_2, among other factors, such as compounds called stress relievers, can trigger the production of specific compounds, influencing functional structures such as vascular tissues. The xylem tracheary elements (TEs) undergo a highly regulated differentiation process involving dedifferentiation, redifferentiation, and programmed cell death, resulting in lignified secondary walls. *Luffa cylindrica*, a Cucurbitaceae, shows elevated investment in growth and vascular differentiation to sustain the high ovary development rates that culminate in large fruits with typical richness in lignocellulosic fibers. We aimed to investigate the morphophysiological, biochemical, and molecular impacts in plants of the target species exposed *in vitro* to Paclobutrazol (PBZ) concentrations (0 – control; 0.21; 0.42; 0.85; 1.7; and 3.4 μM); and to CO_2-enriched atmospheres in open-top chambers {ambient - a[CO_2] (± 400 μM mol^{-1}) and enriched - e[CO_2] (± 800 μM mol^{-1}). Regarding PBZ, as expected, this growth regulator promoted alteration in plant growth, reducing stem and root size. Likewise, the leaves were smaller, more pigmented, and thicker. As a result, the photosynthetic rate decreased at dosages of 1.7 and 3.4 μM of PBZ. In addition, changes in morphology were observed, such as an increase in the area of the vessels of the metaxylem and mesophyll at higher concentrations and the vascular bundle area. PBZ at concentrations of 0.85, 1.7, and 3.4 μM also increased the activity of the antioxidative enzymes, namely Catalase and Peroxidase, as well as lipid peroxidation (as indicated by MDA). There was also an increase in the expression of genes involved in the biosynthesis of polyamines, *Thermospermine synthase* (*LcACL5*), *Polyamine oxidase* (*LcPAO*), *Spermidine synthase* (*LcSPDE*) at the higher concentrations, as well as an increase in *Cinnamyl alcohol dehydrogenase* (*CAD*), involved in the lignin biosynthesis pathway. Regarding CO_2 enrichment, e[CO_2] significantly increased plant height and root length. Over time, there was also an increase in dry and fresh mass, biomass, and specific leaf

area. The analyzed enzymes CAT, SOD, POD, and APX did not change. Concerning sugar content, an increase was observed after 25 days of experimentation with high CO_2. The availability of CO_2 promoted an increase in carbohydrates, which are mobilized for the biosynthesis of essential compounds for plant growth and development. The genes' expression in the lignin (*Cafeato o-methyltransferase - COMT)* and polyamine biosynthesis (*ACL-5*) pathways were positively regulated. These changes in growth and biochemistry allow us to understand that, at high CO_2 concentrations, there is a photosynthetic efficiency that favors the growth and development of this species. The high adaptive efficiency and the reorganization of its metabolism allow this species to survive the future scenario of an environment with high CO_2 concentrations. This study plays an exploratory role in understanding the effects of climate change and its wide-range implications in various areas, such as agricultural adaptations, biodiversity conservation, and human health.

RESUMO

DUTRA, Quezia Pains, D.Sc., Universidade Federal de Viçosa, fevereiro 2024. **Impactos morfofisiológicos em *Luffa cylindrica* (L.) M. Roem. afetada por Paclobutrazol e atmosfera enriquecida com CO_2**. Orientador: Wagner Campos Otoni. Coorientador: Tatiane Dulcineia Silva.

O ciclo de vida das plantas envolve várias estratégias, através da deteção de sinais internos e ambientais, para retomar o crescimento e o desenvolvimento. O ambiente influencia significativamente o metabolismo das plantas, afetando a produção de metabólitos primários e secundários. Altas concentrações de CO_2 atmosférico, entre outros fatores, como os compostos denominados aliviadores de stress, podem desencadear a produção de compostos específicos, influenciando estruturas funcionais como os tecidos vasculares. Os elementos traqueais (ETs) do xilema passam por um processo de diferenciação altamente regulado, envolvendo desdiferenciação, rediferenciação e morte celular programada, resultando em paredes secundárias lignificadas. *Luffa cylindrica*, uma Cucurbitaceae, apresenta elevado investimento em crescimento e diferenciação vascular para sustentar as altas taxas de desenvolvimento do ovário, que culminam em grandes fuitos, com típica riqueza em fibras lignocelulósicas. Objetivamos investigar os impactos morfofisiológicos, bioquímicos e moleculares em plantas da espécie-alvo expostas in vitro a concentrações de Paclobutrazol (PBZ) (0 - controle; 0,21; 0,42; 0,85; 1,7; e 3,4 μM); e a atmosferas enriquecidas com CO_2 em câmaras de topo aberto {ambiente - a[CO_2] (± 400 μM mol^{-1}) e enriquecida - e[CO_2] (± 800 μM mol^{-1}). Em relação ao PBZ, como esperado, este reagente de crescimento promoveu alteração no crescimento das plantas, reduzindo o tamanho do caule e da raiz. Da mesma forma, as folhas eram menores, mais pigmentadas e espessas. Como resultado, a taxa fotossintética diminui sob 1,7 e 3,4 μM de PBZ. Além disso, houve alterações na morfologia, como o aumento da área dos feixes vasculares, dos vasos do metaxilema e do mesofilo nas concentrações de mais elevadas. O PBZ, nas concentrações de 0,85, 1,7 e 3,4 μM, também promoveu aumento nas atividades das enzimas antioxidativas, Catalase e Peroxidase, bem como a peroxidação lipídica (indicada pelo MDA). Verificou-se também aumento da expressão de genes envolvidos na biossíntese de poliaminas, *Termospermina sintase* (*LcACL5*), *Poliamina oxidase* (*LcPAO*), *Espermidina sintase* (*LcSPDE*) nas concentrações mais elevadas, bem do *Cinamil álcool desidrogenase* (CAD), envolvido na via de biossíntese da lignina. Relativamente ao enriquecimento com CO_2,

a e[CO_2] aumentou significativamente a altura das plantas, bem como o comprimento das raízes. Ao longo do tempo, também se registou aumento da biomassa (massas seca e fresca) e da área foliar específica. As enzimas analisadas CAT, SOD, POD e APX não sofreram alterações. Relativamente ao teor de açúcares, observou-se aumento, após 25 dias de experimentação, em e[CO_2]. A disponibilidade de CO_2 promoveu aumento nos carboidratos que são mobilizados para a biossíntese de compostos importantes para o crescimento e desenvolvimento da planta. An expressão de genes envolvidos na via da lignina (*Cafeato o-metiltransferase* - *COMT*) e da biossíntese de poliaminas (*ACL-5*), foram regulados positivamente. Estas alterações no crescimento e na bioquímica permitem-nos compreender que, a altas concentrações de CO_2, existe uma eficiência fotossintética que favorece o crescimento e desenvolvimento desta espécie. A elevada eficiência adaptativa e a reorganização do seu metabolismo permitem a esta espécie sobreviver ao cenário futuro de um ambiente com elevadas concentrações de CO_2. Este estudo tem papel exploratório na compreensão dos efeitos das alterações climáticas e das suas vastas implicações em diversas áreas, como as adaptações agrícolas, a conservação da biodiversidade e a saúde humana.

CONTENTS

GENERAL INTRODUCTION

Over time, plants have developed various mechanisms for their survival. During the stages of their life cycle, various strategies have been acquired for tissue differentiation, pathogen recognition, stress signals, and metabolic status (Iakimova and Woltering, 2017; Birch et al., 2020; Burke et al., 2020; Valandro et al., 2020). For this to happen, genes are signaled and promote programmed cell death events in a controlled and organized manner (Landeo et al., 2021).

The environment reorganizes the plant's metabolism. Depending on the situation imposed, such as an increase in atmospheric CO_2, heat, drought, pathogen attack or a combination of these factors, it affects the production of primary and secondary metabolites in plants (Ahmed et al., 2019; Birami et al., 2020). High CO_2 concentrations can trigger the production of compounds such as alkaloids, lignins, and proline, among others. This can affect functional structures such as the xylem and phloem. To understand these changes, CO_2 enrichment in the open air (FACE) or open-top chambers (OTC) is used.

The tracheary elements (TEs), together with parenchymatous cells and fibers, comprise the vascular tissue (xylem), which is responsible for transporting and distributing water and minerals from the soil to the plant's organs.

TEs are dead, hollow cells with lignified secondary walls. This tissue originates from orderly cell divisions of the procambium and cambium and subsequently, in a highly regulated process, undergoes programmed cell death (PCD) to become functional (Fukuda and Komamine, 1980; Fukuda, 2004; Devillard and Walter, 2014; Iakimova and Woltering, 2017).

The development of TEs *in vitro* includes the isolation of mesophyll cells and their cultivation in a medium containing auxin and/or cytokinins, which induces cell dedifferentiation and makes the cell competent to take on a new differentiation pathway (Fukuda and Komamine 1980; Fukuda, 1997; Buchanan et al., 2015). The redifferentiated cell accumulates hydrolytic enzymes, proteases, Ca^{2+}/CaM, brassinosteroids and deposits secondary wall (Buchanan et al., 2015). Finally, in a process similar to transdifferentiation in vivo (Fukuda, 1997), the tonoplast ruptures, whose content, rich in RNAses, DNAses and proteases, is responsible for the loss of cell content, resulting in a TE consisting solely of a

lignified secondary wall (Buchanan et al., 2015). This event is called xylogenesis (Fukuda, 1997; Demura, 2014; Escamez and Tuominen, 2014).

Xylogenesis is an exquisite, finely regulated event that involves several meticulously structured stages. Thus, the process of PCD and xylem differentiation has been the subject of several studies (Fukuda and Komamine, 1980; Fukuda, 1997; Oda et al., 2005; Pesquet et al., 2010; Pillai et al., 2011). The first study of xylogenesis was carried out on *Zinnia elegans*. In this species, mesophyll cells cultured in a medium containing auxin and cytokinins were induced to transdifferentiate into TEs (Fukuda and Komamine, 1980). With this, the xylogenic culture of *Z. elegans* became a model that allowed a better understanding of hormonal and biochemical signaling and the metabolic and molecular pathways that interact and allow successful transdifferentiation (Iakimova and Woltering, 2017). Since then, this knowledge has been applied to other species (Groover et al., 1997; Kuriyama and Fukuda, 2000; Roberts and McCann, 2000; Oda et al., 2005; Jung et al., 2008; Pesquet et al., 2010; Demura, 2014; Escamez and Tuominen, 2014; Kondo et al., 2015; Fukuda, 2016).

Some compounds can act on the differentiation of these elements, such as PBZ, a triazole that inhibits gibberellin synthesis and abscisic acid catabolism and reduces plant growth. In addition, PBZ minimizes the effects of ethylene, which plays a significant role during programmed cell death events. Studies with PBZ have demonstrated its ability to reorganize metabolism and activate essential pathways for plant growth and development. The changes in phenotype are reduction in plant length, an increase in root diameter, increase in the production of photosynthesizing pigments, increase in sugars, lignin and proline (Win et al., 2017; Ahmad et al., 2015; Soumya et al., 2017; Xu et al., 2017; Xiu et al., 2018).

To understand these mechanisms, studies in an *in vitro* environment can be essential. This system offers a number of advantages for studies involving plant development, as it allows us to follow the stages and understand the various events and mechanisms involved in the development and establishment of the plant body. In addition to practical applications, efficient *in vitro* regeneration protocols help in the study of morpho-anatomical, physiological, biochemical and molecular characters, as well as enabling genetic studies aimed at improving the species (Duclercq et al., 2011; Us-Camas et al., 2014).

Given all this information, there is still a need to fill in gaps and elucidate mechanisms of action in the face of imposed conditions. Species that require xylogenesis for their formation

are strong candidates for understanding cell reorganization in the face of diverse conditions. One species in question is *Luffa cylindrica*, an annual herbaceous species belonging to the Cucurbitaceae family that plays a crucial role in horticulture due to its significant nutritional and economic value. These plants are essential models for understanding plant development principles and improving yield enhancement strategies (Pawełkowicz et al., 2024). It is popularly known as 'bucha', 'esfregão', 'esponja vegetal', 'bucha dos paulistas', 'pepino bravo', 'gonçalinho', 'maxixe do Pará', among others. Native to Asia, it was introduced to Brazil by the Portuguese and is currently grown throughout Brazil, mainly in the state of Minas Gerais (Marouelli et al., 2013; Barroso et al., 2014; Chen et al., 2015). Cell death events occur for its formation, causing a reorganization of the fibres, forming a lignocellulosic structure (Tanobe et al., 2005; Laidani et al., 2012).

REFERENCES

Ahmad P, Jaleel C. A, Azooz MM, Nabi G (2009) Generation of ROS and non- enzymatic antioxidants during abiotic stress in plants. *Botany Research International*, *2*(1), 11–20.

Barroso PA, Rêgo MM, Rêgo ER, Nascimento K.S, Ferreira K.T.C, Santos AA (2014) Caracterização morofológica de plântulas de *Luffa cylindrica* L. germinadas *in vitro*. *Agrotec – Agropecuária Técnica*, 35(1):89-93.

Birch PRJ, Avrova AO, Dellagi A, Lacomme C, Cruz SS, Lyon GD (2018) Programmed cell death in plants in response to pathogen attack. *Annual Review of Plant Biology*, 184–208.

Birami B, Thomas N, Gattmann M, Preisler Y., Gast A, Arneth A, Ruehr N K (2020). Hot drought reduces the effects of elevated CO_2 on tree water- use efficiency and carbon metabolism. *New Phytologist*, *226*, 1607–1621. https://doi.org/10.1111/nph.16471

Buchanan BB, Gruissem W, Jones RL. *Biochemistry and molecular biology of plants.* 2 ed. USA: John Wiley and Sons, Ltd, 2015. 1283p.

Chen X, Tan T, Xu C, Huang S, Tan J, Zhang M, Wang C, Xie C (2015) Genome-wide transcriptome profiling reveals novel insights into *Luffa cylindrica* browning. *Biochemical and Biophysical Research Communications*, 463:1243–1249.

Demura T (2014) Tracheary element differentiation. *Plant Biotechnology Reports*, 8(1):17–21.

Devillard C, Walter C (2014) Formation of plant tracheary elements *in vitro* – a review *New Zealand Journal of Forestry Science*, 44:22-35.

Duclercq J, Sangwan-Norreel B, Catterou M, Sangwan RS (2011) De novo shoot organogenesis: from art to Science. *Trends in Plant Science,* 16:597–606.

Escamez S, Tuominen H (2014) Programmes of cell death and autolysis in tracheary elements: when a suicidal cell arranges its own corpse removal. *Journal of Experimental Botany*, 65(5):1313–1321.

Fukuda H, Komamine A (1980) Establishment of an experimental system for the study of tracheary element differentiation from single cells isolated from the mesophyll of Zinnia elegans. *Plant Physiology* 65:57–60.

Fukuda H (2016) Signaling, transcriptional regulation, and asynchronous pattern formation governing plant xylem development. *Proceedings of the Japan Academy Series B* 92:98–106.

Fukuda H (1997) Tracheary element differentiation. *Plant Cell*, 9(7):1147–1156.

Fukuda H (2004). Signals that control plant vascular cell differentiation. *Nature Reviews Molecular Cell Biology*, 5(5):379–391.

Groover A, De Witt N, Heidel A, Jones A (1997) Programmed cell death of plant tracheary elements differentiating *in vitro*. *Protoplasma,* 196:197–211.

Iakimova ET, Woltwring EJ (2017) Xylogenesis in zinnia (*Zinnia elegans*) cell cultures: unravelling the regulatory steps in a complex developmental programmed cell death event. *Planta*, 245:681–705.

Jung JH, Kim SG, Seo PJ, Park CM (2008) Molecular mechanisms underlying vascular development. *Advances in Botanical Reserch*, 48:1–68.

Kondo Y, Fujita T, Sugiyama M, Fukuda H (2015) A novel system for xylem cell differentiation in *Arabidopsis thaliana*. *Molecular Plant*, 8:612–621.

Kondo Y, Ito T, Nakagami H, Hirakawa Y, Saito M, Tamaki T, Shirasu K, Fukuda H (2014) Plant GSK3 proteins regulate xylem cell differentiation downstream of TDIF- TDR signalling. *Nature Communications*, 5:3504.

Laidani Y, Hanini S, Mortha G, Heninia G (2012) Study of a fibrous annual plant, *Luffa cylindrica* for paper application Part I: Characterization of the vegetal. *Iranian Journal of Chemistry and Chemical Engineering*, 31(4):119–129.

Marouelli WA, Silva HR, Lopes JF (2013) Irrigação na cultura da bucha vegetal. *Embrapa Hortaliças – Circular Técnica*, 16.

Oda Y, Mimura T, Hasezawa S (2005) Regulation of secondary cell wall development by cortical microtubules during tracheary element differentiation in *Arabidopsis* cell suspensions. *Plant Physiology,* 137:1027–1036.

Pawełkowicz M, Zieniuk B, Staszek P, Przybysz A (2024) From Sequencing to Genome Editing in Cucurbitaceae: Application of Modern Genomic Techniques to Enhance Plant Traits. *Agriculture*, *14*(1), 90.

Pesquet E, Korolev AV, Calder G, Lloyd CW (2010) The microtubule-associated protein AtMAP70-5 regulates secondary wall patterning in *Arabidopsis* wood cells. *Current Biology*, 20(8):744–749.

Pesquet E, Ranocha P, Legay S, Digonnet C, Barbier O, Pichon M, Goffner D (2005) Novel markers of xylogenesis in *Zinnia* are differentially regulated by auxin and cytokinin. *Plant Physiology* 139:1821–1839

Pesquet E, Tuominen H (2011) Ethylene stimulates tracheary element differentiation in *Zinnia elegans* cell cultures. *New Phytologist*, 190:138–149.

Pillai KV, McDonald AG, Wagner FG (2011) Developing a model system *in vitro* to understand tracheary element development in Douglas-fir (*Pseudostuga menziesii*). *Maderas Ciencia y Tecnología*, 13(1):3–18.
Roberts K, McCann MC (2000) Xylogenesis: the birth of a corpse. *Current Opinion Plant Biology*, 3:517–522.

Tanobe VOA, Sydenstricker THD, Munaro M, Amico SC (2005) A comprehensive characterization of chemically treated brazilian sponge-gourds (*Luffa cylindrica*). *Polymer Testing*, 24:474–482.

Us-Camas R, Rivera-Solis G, Duarte-Aké F, De-la-Peña C (2014) *In vitro* culture: an epigenetic challenge for plants. *Plant Cell, Tissue and Organ Culture*, 118:187–201.

Valandro F, Menguer PK, Cabreira-Cagliari C, Margis-Pinheiro M, Cagliari A (2020) Programmed cell death (PCD) control in plants: new insights from the *Arabidopsis thaliana* deathosome. *Plant Science*, 110603.

Xiu WY, Zhu Y, Chen B, Hu Y, Dawuda MM (2018) Effects of paclobutrazol on the physiological characteristics of *Malus halliana* Koehne seedlings under drought stress via principal component analysis and membership function analysis. *Arid Land Research and Management,* 1–17.

Xu C, Gao Y, Tian B, Ren J, Meng Q, Wang P (2017) Effects of EDAH, a novel plant growth regulator, on mechanical strength, stalk vascular bundles and grain yield of summer maize at high densities. *Field Crops Research*, 200:71–79.

Chapter 1: Morphophysiological impacts of paclobutrazol on *Luffa cylindrica* (L.) M. Roem. grown *in vitro*

Quezia Pains Dutra[1], Tatiane Dulcineia Silva[1], Michelle Maylla Viana de Almeida[1]; Elisandra da Silva Sousa[1] Auxiliadora Oliveira Martins[2]; Ludmila Nayara de Freitas Correia[1], Juliane Maciel Henschel[3], Kleiton Lima Godoy Machado[1]; Diego Silva Batista[4], Wagner Luis Araújo[2], Wagner Campos Otoni[1]

[1]Department of Plant Biology/Institute of Biotechnology Applied to Agriculture (BIOAGRO), Federal University of Viçosa, 36570-900 Viçosa, MG, Brazil.

[2]Plant Growth Unit, Department of Plant Biology, Federal University of Viçosa, 36570-900 Viçosa, MG, Brazil

[3]Graduate Program in Agronomy (PPGA), Federal University of Paraíba, Areia, PB, 58397-000, Brazil.

[4]Department of Agriculture, Federal University of Paraíba, Campus III, Bananeiras, PB, 58220-000, Brazil.

Abstract

Paclobutrazol (PBZ), a triazole plant growth regulator, modulates various plant hormones, impacting their metabolism and disrupting growth and development. Used in plant tissue culture, PBZ induces stress due to altered osmolarity, humidity, and gas composition. While the effects of PBZ on crops are known, its mechanisms, particularly in delaying senescence, remain unclear. *Luffa cylindrica* L., valued for its lignocellulosic fruits, undergoes significant vascular development, termed xylogenesis. Investigating the influence of PBZ on *L. cylindrica* is essential. This study assessed the morphophysiological responses of in vitro L. cylindrica to PBZ doses. Seeds germinated in half-strength MS medium were transferred to PBZ concentrations (0–3.4 μM). PBZ reduced stem and root size, altered leaf morphology and pigmentation, and decreased photosynthetic rate at higher doses. Morphological changes included increased vessel area and vascular bundle size. PBZ at 0.85–3.4 μM enhanced antioxidative enzyme activity (CAT, POD), lipid peroxidation (MDA), and expression of polyamine biosynthesis genes (LcACL5, LcPAO, LcSPDE), and lignin biosynthesis gene (CAD). Results suggest PBZ induces cellular reorganization through metabolic changes, hormone biosynthesis modulation, and gene activation, impacting growth and development.

Keywords: Anatomy, enzymes, gene expression, triazole, reactive oxygen species, sponge gourd.

Introduction

Plants as sessile organisms have several mechanisms to determine their fate. These processes occur at all stages of the plant life cycle, such as seed maturation, reproduction, formation of vascular elements, and senescence (Praveen et al., 2023). These developmental processes are triggered by signaling cascades, inducing the expression of genes related to several biochemical events that will direct the cell to their fate (Kesawat et al., 2023; Jalili et al., 2022; Li et al., 2023). Since plants are subject to constant abiotic and biotic stresses, events occurring inside the cell can lead to morphological rearrangements or activate defense mechanisms (Asayesh et al., 2023). Such situations can generally lead to a general decrease in the rate of plant cell metabolic activity, membrane depolarization reduced photosynthetic efficiency, and increased production of reactive oxygen (ROS) and nitrogen (NOS) species in the cell (Contreras et al., 2023; Li et al., 2023). When in excess, ROS can activate programmed cell death (PCD) pathways to eliminate cells that have been damaged. In addition to these factors, stress can also be induced, such as the *in vitro* environment, plants are subjected to conditions of high osmolarity, abnormal mineral nutrition, high relative humidity, among others, which can cause changes in development and growth (Gaspar et al., 2002). To minimize some of these effects, some substances, such as triazole compounds, can protect plants against various stresses by increasing the activity of antioxidant enzymes and inducing stress tolerance (Gopi et al., 2007; Soumya et al., 2017). These include paclobutrazol (PBZ), an isoprenoid triazole with plant growth regulating properties. It acts on the levels of plant hormones such as gibberellins (GAs), abscisic acid (ABA), ethylene and cytokinins (Shahzad et al., 2017; Amien et al., 2022). It interferes with gibberellin biosynthesis by inhibiting the oxidation of ent-kaurene to ent-kauronoic acid through the inactivation of cytochrome P450-dependent oxygenase (Gopi and Jaleel, 2009; Rady and Gaballah, 2012), consequently increases the levels of ABA, endogenous cytokines. Thus, it can cause a series of physiological and morphological changes, such as reduction in stem elongation, reduction in leaf area, closure of stomata, accumulation of lignin, reduction in photosynthetic rate, increase in the number of roots, delay in senescence, chlorophyll synthesis, increase in the activity of antioxidant enzymes, among others (Azarcon et al., 2022; Zhao et al., 2023). These statements could be observed in studies in tomato (Shalaby et al., 2022), peanut (Zhao et al., 2023), rice (Maheshwari et al., 2023) and pumpkin (Putri et al., 2022), where PBZ improved the quality of seedlings, increased the amount of ABA,

elevated metabolic activity, guaranteed growth and development of the crop. However, the biochemistry and mechanisms of action are not yet fully elucidated in species grown *in vitro*.

We pose *Luffa cylindrica* (Cucurbitaceae) as a potential species to study the impacts of PBZ on its development and its relationship with changes in its metabolism under *in vitro* condition. It has been widely used in the manufacture of handicrafts, industrial products, folk medicine and for aesthetic purposes (Zhu et al., 2017). Its fibers are used to form biocomposites due to their stiffness (Sahli et al., 2023). In the ripening process, the fruit constitutes a tangle of multidirectionally arranged fibers, composed mainly of cellulose, hemicellulose and lignin, and is therefore called lignocellulosic (Tanobe et al., 2005). The characteristic fibrous appearance of these fruits is due to PCD events that result in the thickening of the secondary wall and lignin accumulation in the parenchyma cells (Zhu et al., 2017). Another characteristic present are the fistulas in the stems that confer efficiency in the hydraulic system, ensuring growth and development even in a xeric environment (Olson, 2005; Ziemmer, 2016). Its vascular tissue originates from ordered cell divisions of the procambium and subsequently, in a highly regulated process, undergoes PCD to become functional (Devillard and Walter, 2014; Iakimova and Woltering, 2017). This process, termed xylogenesis, has been observed in *Zinnia elegans* (Fukuda and Komanine 1980) and *Arabidopsis thaliana* (Pesquet et al., 2010).

Therefore, understanding how PBZ affects the development of *L. cylindrica* can remedy information, fill gaps on morphological modifications, and identify how the gene machinery acts against triazoles. Therefore, the present study aimed to evaluate different doses of PBZ on morphophysiological responses in *L. cylindrica* L., grown *in vitro*.

Materials and Methods

Plant material and experimental design

Mature seeds of *L. cylindrica* purchased from Feltrin Sementes (Farroupilha, RS, Brazil) were mechanically scarified to remove the aryl. Seeds were then immersed in 70% (v/v) ethanol for 1 min, and transferred to a 2.5% (v/v) solution of sodium hypochlorite containing 0.1% (v/v) of Tween 20 for 20 min. Then, the seeds were washed sterile distilled water, and autoclaved at 120 ºC and 108 kPa for 20 min.

Subsequently, the seeds were inoculated in 9 cm-Petri dishes containing 20 mL of MS medium (Murashige and Skoog, 1962) supplemented with 50 mg L^{-1} myo-inositol, 1.5% (w/v) sucrose and 6.5 g L^{-1} agar (PhytoTechnology Laboratories®, Overland Park, KS, USA). The pH of the medium was adjusted to 5.6 ± 0.1. The medium was autoclaved at 120 °C and 108 kPa for 20 min. The cultures were maintained in a growth room at 25 ± 2 °C under a 16 h light photoperiod, under an irradiance of 60 μmol m^{-2} s^{-1} with two LED lamps (AVANT-18W 100-240V 60Hz; LM = 1850 F.P.> 0.92; 6500K (White)), where they remained until the radicle emission, about 3 days.

Seeds with 3-5 mm radicle were transferred to 600 mL glass vials containing 100 mL of MS medium prepared as previously mentioned, but containing 0 – control, 0.21; 0.42; 0.85, 1.7 and 3.4 μmol of PBZ. The flasks were sealed with rigid polypropylene caps with two openings (10 mm diameter) covered with 0.45 μm PTFE membranes (MilliSeal® AVS-045 Air Vent, Tokyo, Japan), allowing a CO_2 exchange rate of 25 μL L^{-1} s^{-1}. After being maintained under light and temperature conditions as mentioned above.

The experiment was conducted in a completely randomized design, with 15 flasks (replicates) containing two explants for each treatment and repeated twice.

Growth parameters

After 15 days of *in vitro* culture, stem length (cm), root length (cm), number of leaves, number of roots, fresh weight (FW) (g), dry weight (DW) (g), and leaf area (cm^2), specific leaf área (cm^2 g^{-1} plants), biomass partitioning (%), and water content (WC) (%) (WC= [(FW – DW) / FW)] x 100, were FW: fresh mass (g) and DW: dry mass (g)) were evaluated. Plant tissues

were collected at the end of the experiment and sectioned into shoot and root. Leaves were detached and fixed individually on white plasticized graph paper. Photographs were taken with a digital camera and images were processed using ImageJ software (Schneider et al., 2012). DW (g) was obtained by oven-drying the plant material at 50 °C for 72 h.

In vitro photosynthetic rate

Gas exchange and *in vitro* photosynthetic rate quantification were performed as proposed by Costa et al. (2014) with some modifications (Silva et al., 2020). Measurements and data collection were performed using an AQ-S151 Infrared CO_2 analyzer (Qubit Systems, Kingston, ON, Canada) and LoggerLite 1.8.1 software (Vernier Software e Technology, Beaverton, OR, USA), respectively. Reference CO_2 was calculated by entering air into an empty flask pumped from the external environment at a constant airflow of 300 mL min^{-1} inside a lighted chamber (blue and red LED lamps). LEDs were connected in a direct current circuit under a voltage of 12 V, formed by two parallel sets of four LEDs connected in series (600 µmol m^{-2} s^{-1}). Plants were kept in darkness for 8 h before analysis. Soon after the reference CO_2 measurement, flasks containing the plants were coupled to the system and the CO_2 was calculated at the stabilization point. Gas exchange was measured by calculating the difference between the reference CO_2 and the CO_2 of plants exposed to atmospheric air. Air temperature and humidity in the balloon were measured by a Spec sensor (Thermo Recorder RS-11; Takai Spec Corp., Aichi, Japan). *In vitro* photosynthetic rate (A) was calculated by the following formula:

$$A\ (\mu mol\ m^{-2}\ s^{-1}) = \frac{\Delta CO_2}{Mol\ Flow}$$

where,

$$\Delta CO_2\ (ppm) = Reference\ CO_2 - Analysis\ CO_2$$

$$Mol\ Flow = \frac{Air\ flow\ rate\ (L\ min^{-1})}{\left(\frac{(Constant\ for\ perfect\ gases\ (22.4)\ X\ Temperature\ (K))}{\frac{60000}{(Leaf\ DW\ per\ plant\ (g))}}\right)}$$

Morphometric analysis

Leaf, stem, and root samples from all PBZ treatments were analyzed for morphometric analysis. For each repetition (n = 4), 10 images were obtained, obtaining a total of 240 images. The parameters evaluated were mesophyll size (μm), bundle size (μm^2), cortex size (μm); metaxylem vessels area (μm^2), and length of palisade cells (μm^2). The software used was ImageJ® version 1.52a (National Institutes of Health, USA) (Abramoff et al., 2004; Collins, 2007).

Anatomical characterization

After 15 days of culture in the induction medium, explants were collected and fixed in 4% glutaraldehyde (Karnovsky 1965). Fixed samples were dehydrated in an ethanolic series, included in methacrylate resin (Historesin, Leica®) and embedded in plastic histomolds (Leica®). Five micrometer thickness cross sections were obtained using an automatic rotary microtome (RM 2155, Leica) and stained using toluidine blue (pH 3.2) for 3 min (O'Brien and McCully, 1981). The specimens were mounted in Permount® (Fisher Chemical™) on glass slides. Images were captured on a light microscope (AX70 TRF; Olympus Optical, Tokyo, Japan) with a U-photo system, coupled to a digital color camera (Spot Insight 3.2.0; Diagnostic Instruments Inc., Sterling Heights, MI, USA) and microcomputer with the Spot Basic image capture program.

Antioxidant activity

Activity of oxidative stress enzymes, superoxide dismutase (SOD), catalase (CAT), peroxidase (POD), and ascorbate peroxidase (APX) was assessed. Briefly, 50 mg of frozen fresh material (aerial part) were homogenizing in 1 mL extraction medium containing 0.1 M potassium phosphate buffer, pH 6.8; 0.1 mM ethylenediaminetetraacetic acid; 1 mM phenylmethylsulfonyl fuoride and 1% (w/v) polyvinylpolypyrrolidone. The samples were vortexed for 10 s, centrifuged at 12,000 rpm for 15 min at 4oC, and the supernatant was removed and set aside on ice for enzyme assays plus protein determination (Bradford, 1976). CAT, APX, and POD activities were determined as proposed previously (Chance and Maehly, 1955; Nakano and Asada, 1981; Havir and McHale, 1987) and expressed as μmol−1 min−1 g−1 protein. SOD activity was measured as described earlier (Giannopolitis and Ries, 1977) and expressed as U min−1 g−1 protein, with 1 U being equivalent to the concentration of SOD

required to inhibit 50% of nitro blue tetrazolium photoreduction *Determination of lipid peroxidation*

Lipid peroxidation was determined based on the quantification of malondialdehyde (MDA), as proposed by Lima et al. (2002) with modifications. Extraction was performed by adding 1 mL of 1% trichloroacetic acid (TCA) to 50 mg of fresh and macerated samples (aerial part). The solution was vortexed and centrifuged at 12,000 × *g* for 15 min at 4 °C. Then, which 125 µL of the supernatant were transferred to new tubes, along with 375 µL of 0.5% 2-thiobarbituric acid (w/v) in 20% TCA (w/v). The reaction proceeded for 30 min with shaking at 95 °C, and was blocked by incubation in an ice bath. The supernatants were transferred to new tubes, centrifuged at 10,000 × *g* for 10 min at 4 ºC, and read on a spectrophotometer at 532 and 600 nm. With the absorbance values, the means of the triplicates were obtained and the MDA concentration was determined by the equation of Heath and Packer (1968), expressing the results in nmol g^{-1} FW.

$$\text{MDA (nmol mL}^{-1}) = \frac{(A_{532} - A_{600}) * 10^6}{155000}$$

Metabolite analysis

Leaf samples (second fully expanded leaf from the apex of the plants) were collected, 12:00 pm (noon). The samples were frozen in liquid nitrogen and subsequently ground for analysis. About 25 mg of freeze-dried tissues were used for extraction with methanol as described and adapted by Lisec et al., (2006). Photosynthetic pigments were determined as described by Wellburn (1994). Carbohydrates (starch, sucrose, glucose and fructose) were assessed as described by Fernie et al., (2001). Soluble total protein was assessed as described by Bradford, (1976) and total amino acid contents were analyzed according to Yemn and Cocking, (1995). Malate content was determined as previously described by Nunes-Nesi et al., (2007). Proline content followed the methodology proposed by Carillo e Gibon, (2011).

RNA extraction, cDNA synthesis, and quantitative PCR analysis

Total RNA was extracted from leaf samples using TRI Reagent® (Sigma-Aldrich Co.), as recommended by the manufacturer. The cDNA was then synthesized using the Superscript™ III kit (Invitrogen, Carlsbad, CA, USA). We evaluated the expression of the gene belonging to the lignin biosynthesis pathway: *Cinnamyl alcohol dehydrogenase* (*PgCAD*) (Batista et al., 2019) and genes designed based on the *L. cylindrica* transcript: *Thermospermine synthase* (*LcACL5*), *Polyamine oxidase* (*LcPAO*), *Spermidine synthase* (*LcSPDE*) were evaluated. The *40S ribosomal protein S9 gene* (*BoRPS9*) was used for normalization (Moreira et al., 2018). Expression analyses were performed by real-time PCR on a CFX96 Touch™ device (BIO-RAD) using SYBR Green Master Mix (BIO-RAD), the reactions were performed with four biological replicates each in duplicate technique, in a reaction volume of 10 µL (4 µL of SYBR-Green, 0.2 µL of each primer, 3.6 µL of diethylpyrocarbonate-treated water and 2 µL (40 ng) of cDNA. The amplification conditions were carried out in the following steps: 2 min at 50 ºC and 10 min at 95 ºC, followed by 40 cycles of 95 ºC for 15 s and 60 ºC for 60 s, and the dissociation curve from 60 to 95 ºC at 0.5 ºC s^{-1}. Transcription levels were determined using the $2^{-\Delta\Delta Ct}$ method (Livak and Schmittgen, 2001), with three biological replicates with at least two technical replicates each.

Statistical analysis

Statistical analysis was performed using software Genes (Cruz, 2013). Experiments were repeated twice. Data were submitted to one-away analysis of variance (ANOVA) and means were compared by Dunnet test at 5% significance.

Results

Paclobutrazol alters biomass accumulation and photosynthetic rate

PBZ reduced plant growth compared to control plants (Figs. 1 and 2). There was a more than 2-fold increase in the fresh weight of the leaves of plants subjected to concentrations higher than 0.42 µM of PBZ, compared to the control (Fig. 3d). On the other hand, there was a great reduction in the total and specific leaf area of plants grown at all doses of PBZ, which can reach almost 5-fold to 3.4 µM of PBZ (Figs. 3a and b). In addition, 1.7 and 3.4 µM of PBZ reduced the number of leaves, which consequently promote reduction in the dry mass of the leaves, compared to the control (Fig. 2c and e, respectively).

All doses of PBZ reduced stem height, while stem dry mass was reduced by 0.42; 0.85; 1.7 and 3.4 µM of PBZ and stem fresh mass was reduced by 1.7 and 3.4 µM of PBZ (Figs. 2f, g and h, respectively). Reductions of up to 16-fold in root length were also observed at all doses (Fig. 3i) and in root fresh weight (0.85; 1.7 and 3.4 µM of PBZ) (Fig. 3j). For the variables root dry mass and root number, no difference was observed when compared to the control (Figs. 3k and l).

More biomass was allocated to the leaves under up to 0.85 µM of PBZ, reducing the biomass allocated to the stems and roots (Fig. 4c). Concomitantly with the lower plant growth, there was a significant decrease in photosynthetic rate in plants grown with 3.4 µM of PBZ, although there has been a tendency of gradative reduction since the lower concentration (Fig. 4a). Similarly, to what was observed in the fresh leaf mass, the water content of the leaf showed gradual increases with the increase in the PBZ dose, with this increase being significant from 0.85 µM of PBZ (Fig. 4b).

Hight dose of PBZ triggers generation of oxidative stress in L. cylindrica plants.

Compared to control, 1.7 and 3.4 µM of PBZ increased POD activity and MDA content (Fig 4d-f). Similarly, a significant increase was observed for CAT activity in plants exposed at 0.85, 1.7 and 3.4 µM of PBZ (Fig 4b). These results demonstrate that exposure of *L. cylindrica* to high concentrations of PBZ triggers the generation of oxidative stress. However, there were no significant differences to SOD and APX activities, also to H_2O_2 contents (Fig. 4a, c and e).

PBZ induced morphoanatomical changes in L. cylindrica in the microscopy analysis

We observed morphological changes in the leaves of *in vitro* plants submitted to PBZ (Figs. 6, 7 and 8). The leaves consist of uniseriate epidermis, large central vascular bundle with parenchyma distributed along the main vein, subepidermal collenchyma and dorsiventral mesophyll, subdivided into palisade and spongy parenchyma (Fig. 6). However, plants submitted to PBZ showed different characteristics. We observed an increase in mesophyll size with increasing PBZ concentration (Table 1). In addition, the palisade parenchyma had two or more layers and changes in cell shape, and in the spongy parenchyma there were no intercellular spaces (Fig. 6f, i, l, o and r). The size of the vascular bundle decreased by 3.4 µM and that of the metaxylem vessels decreased significantly when the plants were subjected to 1.7 and 3.4 µM of PBZ, respectively (Table 1). The length of the palisade cells increased from the 0.42 µM concentration of PBZ (Table 1).

Stems in all treatments showed uniseriate epidermis, subepidermal collenchyma, hollow pith and 6 ring-shaped medullary bundles (Fig. 7). The phloem and xylem are arranged in vascular bundles that constitute a bicollateral type vascular subunit, where the phloem on both sides of the xylem (Fig. 7). An increase in the size of vascular bundles was observed as the PBZ dosages increased (Figs. 7 c-l; Table 1). In roots, we found that PBZ increased cortex size and reduced intercellular spaces (Figs. 8 c-l; Table 1). The xylem development was visually more pronounced with increasing PBZ concentration compared to control plants (Fig. 8 k-l). In conjunction with the significant increase in metaxylem vessels in plants grown under 3.4 µM of PBZ (Table 1).

PBZ affects metabolite levels on the nitrogen and carbon metabolism

Primary metabolism compounds such as proteins, starch, sugar (glucose, fructose, sucrose) and amino acids were influenced by PBZ (Figs. 9 and 10). There was a 2-14-fold increase for glucose and fructose and a 1-4-fold increase for sucrose when compared to the control. It is worth mentioning that this increase was gradual according to the increase in PBZ concentration. Although there was a tendency for increases in starch content as the PBZ concentration increased, only at concentrations of 1.7 and 3.4 µM of PBZ were significant differences detected when compared to the control (Fig. 9d). At dosages higher to 0.21 µM of PBZ, the proline content increased significantly compared to the control (Fig. 10c). The same

behavior we also observed when we evaluated the total amino acid levels in all treatments compared to the control, where verified an increase from 5 to 10-fold (Fig. 10d). However, malate and protein content did not differ significantly between treatments (Figs. 10a-b). The highest concentration showed an increase in total phenols compared to the control (Fig. 10e). Concerning pigments, there was an increase in chlorophyll a in the treatments with 0.85; 1.7 and 3.4 µM of PBZ and in chlorophylls b and carotenoids in 3.4 µM of PBZ compared to the control (Figs. 11 a, b and c). Consequently, there was an increase in total chlorophylls at dosages 1.7 and 3.4 µM (Fig.11d). However, the chlorophyll *a*/*b* ratio did not differ significantly compared to the control (Fig. 11e).

PBZ modulated the expression of genes related to the lignin and polyamine biosynthetic pathway

In the phenylpropanoid and polyamine biosynthesis pathway, the expression of the *Cinnamyl alcohol dehydrogenase* (*PgCAD*) and *Polyamine oxidase* (*LcPAO*) genes was positively influenced by PBZ. At concentrations of 0.42, 0.85 and 3.4 µM of PBZ there was a 2-3-fold increase compared to the control (Figure 12c). The LcACL5 gene, compared to the control, had an 8-fold increase at concentrations of 0.42 and 0.85 and 3.4 µM of PBZ (Figure 12a). In contrast, the LcSPDE gene had a 1.5, 4 and 6-fold increase at concentrations of 0.42, 0.85 and 3.4 µM PBZ, respectively, compared to the control (Fig. 12d).

Discussion

This study investigated the effects of PBZ on the morphophysiological responses of *L. cylindrica* grown *in vitro*. PBZ acts on slow leaf growth and increases water retention, making the leaves appear heavier in terms and more compact in terms of fresh mass. These statements align with Colado and Hernandez (2022), whose results indicated a smaller leaf area, a larger mesophyll, an increase in fresh mass and a decrease in leaf dry mass. As a result of the smaller leaf area, the photosynthetic rate was reduced by up to 2.5 times.

On the other hand, an increase in specific leaf area was observed, demonstrating that, despite a lower photosynthetic rate, its efficiency is maintained. Morpho-anatomical characteristics were also affected with the increase in PBZ concentration, such as a more pronounced vascular system with greater differentiation of the xylem and an increase in the size of the cortex. Some studies have reported a compensatory system in which the reduction in leaf area may be associated with an increase in cell division, which allows the chloroplast density to be adjusted in order to modulate the photosynthetic rate (Ferjani et al., 2007; Jiang et al., 2012).

Triazoles are compounds that alter the morphology and metabolism of plants. Among these, PBZ alters the balance of important plant hormones, such as GAs, ABA, ethylene and cytokinins. These hormones are important throughout the plant's life cycle to maintain physiological and morphological functions (Li et al., 2023). By blocking the biosynthesis of GAs, PBZ inhibits cell elongation, which explains the reduced growth of *L. cylindrica* observed here. This reduction in cell elongation was further confirmed by the smaller diameter of the cells (Redemacher, 2000) under PBZ. Stunted plant growth after PBZ treatment has also been observed in *Curcumis sativus* (Orabi et al., 2010), *Zea mays* (Kamran et al., 2017), *Raphanus sativus* (Henschel et al., 2021), *Solanum tuberosum* (Hou et al., 2022) and *Oryza sativa* (Azarcon et al., 2022).

PBZ altered leaf morphology, with thicker laminae, smaller leaf area, thicker epidermis and greater density of vascular bundles, and palisade parenchyma with elongated layers. These affirmations can be seen in the present study and as reported by Araujo et al. (2019), Lailaty and Nugroho (2021) and Tsegaw et al. (2005). PBZ increases endogenous cytokinin levels, which raises chlorophyll levels and decreases intercellular CO_2 concentration (Zhu et al., 2004; Darussalam and Kumala, 2022). Consequently, these events cause the leaves to turn dark green and increase the activity of some antioxidant enzymes. Although PBZ reduces growth as a

whole, the most significant impact is on leaves and stems since these require high levels of GA to trigger responses (Henschel et al., 2021; Li et al., 2023). In roots, it promotes abnormal thickening due to increased cortical cells (Tanimoto, 2012). According to Weng et al. (2015), there was an increase in root diameter and a greater number of roots in the PBZ treatments. This data could be observed in the present study with an increase in the vascular bundle and the number of roots. For these phenotypic responses to occur, several biochemical changes take place, such as an increase in proline (Yang et al., 2019), chlorophyll and carotenoids (Nivedithadev et al., 2012), polyamines (Bindu et al., 2017) and soluble carbohydrates (Ghasemi et al., 2014). This indicates that PBZ causes a change in plant homeostasis and that even with the reduction in photosynthetic rates, metabolites still provide energy to feed metabolic demands and alleviate the effects of reactive oxygen species (ROS). This can be seen in this study with the increase in sugars, chlorophylls *a* and *b*, amino acids, and proline.

Our results indirectly showed that PBZ can increase the production of ROS, since we observed an increase in the activity of antioxidant enzymes, such as CAT and POD, and membrane damage, suggested by the increase in MDA production. ROS are directly produced by redox metabolic reactions linked to various processes, such as PCD, and can act as signals that activate secondary metabolic pathways and programmed gene expression networks that lead to various events (Bresson et al., 2018; Waszczak et al., 2018; Khan et al., 2023). Excessive ROS production can lead to senescence and autophagy in plants, causing permanent damage to macromolecules (Altaf et al., 2020; Bhatla et al 2023). To mitigate this phenomenon, the antioxidant deactivation machinery is activated (Gill and Tuteja, 2010), and these processes are modulated through the biosynthesis of PCD, the activation of polyamine synthesis and various hormones. The process occurs when the membrane is depolarized and cellular contents are leaked and membrane lipids are degraded, leading to lipid peroxidation. In turn, CAT and APX can act as detoxification agents and play an important role in reducing oxidative damage induced by ROS (Kesawat et al., 2023).

On the other hand, other events take place so that the plant's biochemistry is not affected. The complex interaction between ABA, NO and polyamines triggers a cascade of molecular events that orchestrate a series of plant protective responses. These responses include the regulation of ion channels, the modulation of the stomatal response (which partly involves hydrogen peroxide - H_2O_2), the activation of antioxidant enzymes (partly mediated by nucleoside diphosphate kinase - NDPK), the synthesis of osmolytes (such as amino acids and other compounds) and the differential regulation of gene expression (Shi and Chan, 2014;

Andronis et al., 2014). Studies by Tisi et al. (2011) have shown that H_2O_2 derived from polyamine synthesis serves as a signal for secondary wall deposition and programmed cell death. These statements could be seen in the present study with the increased expression of the PAO and SPDE genes as the concentration of PBZ increased, demonstrating the reorganization of *Luffa* metabolism.

In addition to changes in metabolism, PBZ can alter the levels of plant hormones and, consequently, affect the size of the xylem and phloem. According to Opio et al. (2020), adding PBZ to plants can increase auxin levels. This is due to the accumulation of non-structural carbon, such as starch (Zheng et al., 2012) simultaneously with a decrease in gibberellins. In studies carried out by Sahoo et al. (2022) with the mango crop, a reduction in the vascular bundles in the root was observed, affecting its growth rate and a reduction in the spongy parenchyma in the leaves. However, although there was a reduction in xylem, they observed an increase in phloem (Murti et al., 2001). Halfizee et al. (2016) observed that in seedlings of *Elaeis guineensis* Jacq. the cells of the stem cortex decreased. This increase in endogenous auxin levels may be related to an increase in the expression of genes related to xylem differentiation and procambial divisions, such as *ACL5*, which, depending on the situation the plant is in, slows down xylem growth (Ayvaci et al., 2023). According to Hanzawa et al. (2000) in studies with Arabidopsis, the addition of auxins increased *ACL5* transcription levels. In a study by Iakimova and Woltering (2017) in which the process of xylogenesis in *Zinnia* was observed, it was shown that endogenous polyamines stimulate xylem differentiation and that *ACL5* prevents premature xylem death. According to Muñiz et al. (2008), through the anatomical characterization of the hypocotyl of Arabidopsis thaliana, they observed that mutations in the putative *ACL5* gene affected the development of the xylem and lacked fibers. Furthermore, the presence of *ACL5* helps in the processes of xylogenesis.

Conclusion

This study comprehensively explored the effects of PBZ on morphophysiological responses of *L. cylindrica in vitro*. It demonstrated significant impacts on leaf growth dynamics and notable morpho-anatomical changes, including enhanced vascular development and cortex growth. These findings align with previous research, indicating consistent influence of PBZ on plant anatomy. Moreover, biochemical analysis revealed PBZ's disruption of hormonal balance,

inhibiting cell elongation and resulting in reduced growth and cell size, consistent with observations in other plant species. Overall, this research underscores the intricate effects of PBZ on *L. cylindrica* morphophysiology, emphasizing the importance of understanding regulator-plant interactions for sustainable agriculture.

References

Azarcon, R. P., Vizmonte Jr, P. T., Agustin, A. M. L. (2022). Effects of paclobutrazol on growth, yield and water use efficiency of rice (*Oryza sativa* L.) under drought stress condition. *Mindanao Journal of Science and Technology*, *20*(1).

Altaf, M.M., Diao, X-p., ur Rehman, A. et al. Effect of Vanadium on Growth, Photosynthesis, Reactive Oxygen Species, Antioxidant Enzymes, and Cell Death of Rice (2020). *Journal of Soil Science and Plant Nutrition*, *20*, 2643–2656. https://doi.org/10.1007/s42729-020-00330-x

Abramoff, M. D., Magalhães, P. J., Ram, S. J. (2004). Image processing with ImageJ. *Biophotonics International*, *11*(7):36–42.

Andronis, E. A., Moschou, P. N., Toumi, I., Roubelakis-A, K. A. (2014). Peroxisomal polyamine oxidase and NADPH-oxidase crosstalk for ROS homeostasis which affects respiration rate in *Arabidopsis thaliana*. *Frontiers in Plant Science*, *5*, 132.

Asayesh, Z. M., Arzani, K., Bidgoli, M.-A., Abdollahi, H. (2023). Enzymatic and non-enzymatic response of grafted and ungrafted young European pear (*Pyrus communis* L.) trees to drought stress. *Scientia Horticulturae*, *310*, 111745.

Amien, S., Aini, Q., Wicaksana, N. (2022). Effect of paclobutrazol on growth and root morphology of 12 crossed stevia *in vitro*. *Kultivasi*, *21*(2).

Araujo, F. F., Santos, M. N., Costa, L. C., Moreira, K. F., Araujo, M. N., Martinez, P. A., e Finger, F. L. (2019). Changes on potato leaf metabolism and anatomy induced by plant growth regulators. *Journal of Agricultural Science*, *11*(7):139–147.

Ayvaci, U., Koc, F.N., Cetinkaya, H. *et al* (2023). Treatment with auxin and paclobutrazol mediates ROS regulation, antioxidant defence system and cell wall response in salt treated soybean. *Brazilian Journal of Botany*. https://doi.org/10.1007/s40415-023-00922-8.

Ahmad, P., Jaleel, C. A., Azooz, M. M., Nabi, G. (2009). Generation of ROS and non-enzymatic antioxidants during abiotic stress in plants. *Botany Research International*, *2*(1),11–20.

Bates, L. S., Waldren, R. P., Teare, I. D. (1973). Rapid determination of free proline for water-stress studies. *Plant and Soil*, *39*(1), 205–207.

Batista, D. S., Moreira, V. S., Felipe, S. H. S., Fortini, E. A., Silva, T. D., Chagas, K., Louback, E., Romanel, E., Costa, M. G. C., Otoni, W. C. (2019). Reference gene selection for qRT-PCR in Brazilian-ginseng [*Pfaffia glomerata* (Spreng.) Pedersen] as affected by various abiotic factors. *Plant Cell, Tissue and Organ Culture*, *138*(1), 97– 107.

Bindu, G.V., Sharma, M., Upreti, K.K. (2017). Polyamine and ethylene changes during floral initiation in response to paclobutrazol in mango (*Mangifera indica* L.). *International Journal of Environmental e Agriculture Research,* 3: 34–40.

Birami, B., Nägele, T., Gattmann, M., Preisler, Y., Gast, A., Arneth, A., Ruehr, N. K. (2020). Hot drought reduces the effects of elevated CO_2 on tree water-use efficiency and carbon metabolism. *New Phytologist*, *226*(6), 1607–1621. https://doi.org/10.1111/nph.16471

Bhatla, S.C., Lal, M.A. (2023). Senescence and Programmed Cell Death. In: *Plant Physiology, Development and Metabolism. Springer, Singapore*. https://doi.org/10.1007/978-981-99-5736-1_30.

Bresson, J., Bieker, S., Riester, L., Doll, J., Zentgraf, U. (2018). A guideline for leaf senescence analyses: from quantification to physiological and molecular investigations. *Journal of Experimental Botany*, *69*(4), 769–786.

Cruz, C. D. (2013). Genes: a software package for analysis in experimental statistics and quantitative genetics. *Acta Scientiarum. Agronomy*, *35*, 271–276.

Costa, A.C., Rosa M., Megguer, C.A., Silva, F.G., Pereira, F.D., Otoni, W.C. (2014). A reliable methodology for assessing the *in vitro* photosynthetic competence of two Brazilian savanna species: *Hyptis marrubioides* and *Hancornia speciosa. Plant Cell, Tissue and Organ Culture*, *117*, 443–454.

Chance, B., Maerhly, A.C. (1955). Assay of catalases and peroxidases. *Methods in Enzymology, 2*, 764–775. Doi: 10.1016/S0076-6879(55)02300-8.

Collado, C. E., Hernández, R. (2022). Effects of light intensity, spectral composition, and paclobutrazol on the morphology, physiology, and growth of petunia, geranium, pansy, and dianthus ornamental transplants. *Journal of Plant Growth Regulation*, *41***,** 461–478.

Contreras, A. L. A., Emus, A., Gutierrez, E. P., Heredia, J. B. (2023). Stressed Plants: An Improved Source for Bioactive Phenolics. In: *Plant Phenolics in Abiotic Stress Management* (pp. 195-214). Singapore: Springer Nature Singapore.

Cui, L., Zou, Z., Zhang, J., Zhao, Y.,Yan, F. (2016). 24-Epibrassinoslide enhances plant tolerance to stress from low temperatures and poor light intensities in tomato (*Lycopersicon esculentum* Mill.). *Functional and Integrative Genomics*, *16*, 29–35.

Collins, T. J. (2007). ImageJ for microscopy. *Biotechniques*, *43*(S1), S25–S30.

Cruz, C. D. (2016). Genes Softwar- extended and integrated with the R, Matlab and Selegen. *Acta Scientiarum. Agronomy*, *38*(4), 547.

Devillard, C., Walter, C. (2014). Formation of plant tracheary elements *in vitro*–a review. *New Zealand Journal of Forestry Science*, *44*(1), 22.

Darussalam, D., Dewi, K. (2022). Paclobutrazol and Cytokinin Regulation on Culm Growht of Black Rice (*Oryza sativa* L. "Cempo Ireng"). *Bioeksperimen: Jurnal Penelitian Biologi*, *8*(2), 121–128.

Fernie, A. R., Roscher, A., Ratcliffe, R. G., Kruger, N. J. (2001). Fructose 2,6-bisphosphate activates pyrophosphate: fructose-6-phosphate 1-phosphotransferase and increases triose phosphate to hexose phosphate cycling in heterotrophic cells. *Planta*, *212*(2), 250–263.

Fernie, A. R., Roscher, A., Ratcliffe, R. G., Kruger, N. J. (2001). Fructose 2,6-bisphosphate activates pyrophosphate: fructose-6-phosphate 1-phosphotransferase and increases triose phosphate to hexose phosphate cycling in heterotrophic cells. *Planta, 212*(2), 250–263. https://doi.org/10.1007/s004250000386.

Fletcher, R. A., Gilley, A., Sankhla, N., Davis, T. D. (2000). Triazoles as plant growth regulators and stress protectants. *Horticultural Reviews*, *24*, 55–138.

Fukuda H, Komamine A (1980). Establishment of an experimental system for the study of tracheary element differentiation from single cells isolated from the mesophyll of *Zinnia elegans*. *Plant Physiology* 65:57–60.

Gaspar T, Franck, T, Bisbis, B, Kevers, C, Jouve, L, Hausman, J. F, Dommes, J. (2002). Concepts in plant stress physiology. Application to plant tissue cultures. *Plant Growth Regulation*, *37*, 263–285.

Gopi, R., Jaleel, C. A., Panneerselvam, R. (2008). Leaf anatomical responses of *Amorphophallus campanulatus* to triazoles fungicides. *EurAsian Journal of BioSciences*, *2*.

Gill, S. S., Tuteja, N. (2010). Reactive oxygen species and antioxidant machinery in abiotic stress tolerance in crop plants. *Plant Physiology and Biochemistry*, *48*(12), 909–930.

Ghasemi Soluklui, A. A., Ershadi, A., Tabatabaee, Z. E., Fallahi, E. (2014). Paclobutrazol-induced biochemical changes in pomegranate (*Punica granatum* L.) cv. 'Malas Saveh'under freezing stress. *International Journal of Horticultural Science and Technology*, *1*(2), 181–190.

Havir, E. A., McHale, N. A. (1987). Biochemical and developmental characterization of multiple forms of catalase in tobacco leaves. *Plant Physiology*, *84*(2), 450–455.

Hafizee, M. N. (2016). Impact of paclobutrazol on the growth and development of nursery grown clonal oil palm (*Elaeis guineensis* Jacq.) *Journal of Oil Palm Research*, 28, 404–414.

Häuser, C., Kwiatkowski, J., Rademacher, W., Grossmann, K. (1990). Regulation of endogenous abscisic acid levels and transpiration in oilseed rape by plant growth retardants. *Journal of Plant Physiology*, *137*(2), 201–207.

Hanzawa, Y., Takahashi, T., Michael, A. J., Burtin, D., Long, D., Pineiro, M., Coupland, G. and Komeda, Y. (2000). *ACAULIS5,* an *Arabidopsis* gene required for stem elongation, encodes a spermine synthase. *EMBO Journal*19, 4248–4256.

Henschel, J.M., Brito, F.A., Pimenta, T.M., Picoli, E.A., Zsögön, A., Ribeiro, D.M. (2021) Irradiance-regulated biomass allocation in *Raphanus sativus* plants depends on gibberellin biosynthesis. *Plant Physiology and Biochemistry*, *168*, 43–52.

Hou, Y. X., Hu, Y. S., Chen, C. M., Wu, H. C. (2022). Growth of Potato Plantlets in Response to Ventilation, Sucrose, and Paclobutrazol in Modified Temporary Immersion Vessels. *HortScience*, *57*(11), 1424–1429.

Iakimova, E. T., Weltering, E. J. (2017). Xylogenesis in zinnia (*Zinnia elegans*) cell cultures: unravelling the regulatory steps in a complex developmental programmed cell death event. *Planta*, *245*, 681–705. https://doi.org/10.1007/s00425-017-2656-1

Jalili, S., Ehsanpour, A. A., Javadirad, S. M. (2022). The role of melatonin on caspase-3-like activity and expression of the genes involved in programmed cell death (PCD) induced by *in vitro* salt stress in alfalfa (*Medicago sativa* L.) roots. *Botanical Studies*, *63*(1), 19.

Karnovsky MJ (1965). A formaldehyde-glutaraldehyde fixative of high osmolality for use in electron microscopy. *The Journal of Cell Biology* 27: 137-138.

Khan, M., Ali, S., Al Azzawi, T. N. I., Saqib, S., Ullah, F., Ayaz, A., Zaman, W. (2023). The key roles of ROS and RNS as a signaling molecule in plant–microbe interactions. *Antioxidants*, *12*(2), 268.

Kamran, M., Wennan, S., Ahmad, I. et al. (2018). Application of paclobutrazol affect maize grain yield by regulating root morphological and physiological characteristics under a semi-arid region. *Scientific Reports 8*, 4818. https://doi.org/10.1038/s41598-018-23166-z.

Kesawat, M. S., Satheesh, N., Kherawat, B. S., Kumar, A., Kim, H. U., Chung, S. M., Kumar, M. (2023). Regulation of Reactive Oxygen Species during Salt Stress in Plants and Their Crosstalk with Other Signaling Molecules—Current Perspectives and Future Directions. *Plants*, *12*(4), 864.

Kuai, J., Sun, Y., Zhou, M., Zhang, P., Zuo, Q., Wu, J., Zhou, G. (2016). The effect of nitrogen application and planting density on the radiation use efficiency and the stem lignin metabolism in rapeseed (*Brassica napus* L.). *Field Crops Research*, *199*, 89–98.

Khan, M. S., Hemalatha, S. (2022). Autophagy and programmed cell death are critical pathways in Jasmonic acid mediated saline stress tolerance in *Oryza sativa*. *Applied Biochemistry and Biotechnology*, *194*(11), 5353–5366.

Lailaty, I. Q., Nugroho, L. H. (2021). Vegetative anatomy of three potted Chrysanthemum varieties under various paclobutrazol concentrations. *Biodiversitas Journal of Biological Diversity*, *22*(2).

Lisec, J., Schauer, N., Kopka, J., Willmitzer, L., Fernie, A.R. (2006). Gas chromatography mass spectrometry-based metabolite profiling in plants. *Nature Protocols*, *1*(1), 387

Liu, B., Long, S., Liu, K., Zhu, T., Gong, J., Gao, S., Xu, Y. (2022). Paclobutrazol Ameliorates Low-Light-Induced Damage by Improving Photosynthesis, Antioxidant Defense System, and Regulating Hormone Levels in Tall Fescue. *International Journal of Molecular Sciences*, *23*(17), 9966.

Li, J., Peiyue, X. Baohong, Z., Yanyan, S., Shizhi, W., Yujie, B., Li, J., Yong, L., Gongxiu, H., Zhang, D. (2023). "Paclobutrazol Promotes Root Development of Difficult-to-Root Plants by Coordinating Auxin and Abscisic Acid Signaling Pathways in Phoebe bournei" *International Journal of Molecular Sciences, 24* (4), 3753. https://doi.org/10.3390/ijms24043753.

Maheshwari, C., Garg, N. K., Singh, A., Tyagi, A. (2023). Optimization of paclobutrazol dose for mitigation of water-deficit stress in rice (*Oryza sativa* L.). *Biochemical Systematics and Ecology*, *107*, 104596.

Mackay, C. E., Hall, J. C., Hofstra, G., Fletcher, R. A. (1990). Uniconazole-induced changes in abscisic acid, total amino acids, and proline in *Phaseolus vulgaris*. *Pesticide Biochemistry and Physiology*, *37*(1), 74–82.

Maxwell, K., Johnson, G. N. (2000). Chlorophyll fluorescence—a practical guide. *Journal of Experimental Botany*, *51*(345), 659–668.

Moreira, V. S., Soares, V. L., Silva, R. J., Sousa, A. O., Otoni, W. C., Costa, M. G.C. (2018). Selection and validation of reference genes for quantitative gene expression analyses in various tissues and seeds at different developmental stages in *Bixa orellana* L. *Physiology and Molecular Biology of Plants*, *24*, 369–378.

Murashige, T., Skoog, F. (1962). A revised medium for rapid growth and bio assays with tobacco tissue cultures. *Physiologia Plantarum*, *15*(3): 473–497.

Muñiz, L., Eugenio G., Minguet, Sunil K S., E Pesquet., Sirera F V., Charleen L. MoreauC., Juan C., Miguel A. B., HTuominen. (2008); ACAULIS5 controls Arabidopsis xylem specification through the prevention of premature cell death. *Development*; *135* (15): 2573–2582. Doi: hpps://doi.org/10.1242/dev.019349.

Neff, M. M., Chory, J. (1998). Genetic interactions between phytochrome A, phytochrome B, and cryptochrome 1 during *Arabidopsis* development 1. *Plant Physiology*, *118*(1), 27–35.

Nivedithadevi, D., Somasundaram, R., Pannerselvam, R. (2012). Effect of abscisic acid, paclobutrazol and salicylic acid on the growth and pigment variation in *Solanum trilobatum* (L.). *International Journal of Drug Development and Research*, *4*(3), 236–246.

O'Brien, T.P., McCully, M.E. (1981) The study of plant structure principles and select methods. Melbourne: *Termacarphi Ltda,* 56–58.

Olson, M. E. (2005). Wood, bark, and pith anatomy in Pittocaulon (∼ Senecio, Asteraceae): Water storage and systematics1. *The Journal of the Torrey Botanical Society*, *132*(2), 173–186.

Opio, P., Tomiyama, H., Saito, T., Ohkawa, K., Ohara, H., Kondo, S. (2020). Paclobutrazol elevates auxin and abscisic acid, reduces gibberellins and zeatin and modulates their transporter genes in Marubakaido apple (*Malus prunifolia* Borkh. var. Ringo Asami) rootstocks. *Plant Physiology and Biochemistry*, *155*, 502–511.

Orabi, S.A., Salman, S.R., Shalaby, M.A.F (2010) Increasing resistance to oxidative damage in cucumber (*Cucumis sativus* L.) plants by exogenous application of alicylic Acid and Paclobutrazol. *World Journal of Agricultural Sciences*, *6*(3):252–259.

Pawełkowicz, M., Zieniuk, B., Staszek, P., Przybysz, A. (2024). From Sequencing to Genome Editing in Cucurbitaceae: Application of Modern Genomic Techniques to Enhance Plant Traits. *Agriculture*, *14*(1), 90.

Pennell, R.I., Lamb, C. (1997). Programmed cell death in plants. *The Plant Cell*, *9*(7), 1157.

Pesquet, E., Jauneau, A., Digonnet, C., Boudet, A.M., Pichon, M., Goffner, D. (2003). *Zinnia elegans*: the missing link from *in vitro* tracheary elements to xylem. *Physiologia Plantarum*, *119*(4), 463–468.

Praveen, A., Dubey, S., Singh, S., Sharma, V. K. (2023). Abiotic stress tolerance in plants: a fascinating action of defense mechanisms. *3 Biotech*, *13*(3), 102.

Pesquet, E., Korolev, A.V., Calder, G., Lloyd, C.W. (2010). The microtubule-associated protein AtMAP70-5 regulates secondary wall patterning in Arabidopsis wood cells. *Current Biology*, *20*(8), 744–749.

Putri, R.H., Purwantoro, A., Handayani, V.D.S., Respatie, D.W. (2022). Effects of paclobutrazol concentrations and watering frequencies on the flowering ratio of cucumber plants (*Cucumis sativus* L.). *Ilmu Pertanian (Agricultural Science)*, *7*(1).

Porra, R.J., Thompson, W.A., Kriedemann, P.E. (1989). Determination of accurate extinction coefficients and simultaneous equations for assaying chlorophylls a and b extracted with four different solvents: verification of the concentration of chlorophyll standards by atomic absorption spectroscopy. *Biochimica et Biophysica Acta (BBA) - Bioenergetics*, 975(3), 384–394. https://doi.org/10.1016/S0005-2728(89)80347-0.

Rademacher, W. (2000). Growth retardants: effects on gibberellin biosynthesis and other metabolic pathways. *Annual Review of Plant Biology*, *51*(1), 501–531.

Reape, T. J., Molony, E. M., McCabe, P. F. (2008). Programmed cell death in plants: distinguishing between different modes. *Journal of Experimental Botany*, *59*(3), 435–444.

Sahoo, M. R., Kishore, K., Dash, D. K., Panda, C. M., Panda, R. K., Nayak, P. K. (2022). Influence of paclobutrazol on growth, root traits, anatomical modifications and leaf nutrient status in mango. *Journal of Environmental Biology*, *43*(3), 468–476.

Silva, T.D., Batista, D.S., Fortini, E.A., Castro, K.M.,Felipe, S.H.S.; Fernandes, A.M.; de Jesus Sousa, R.M.; Chagas, K.; da Silva, J.V.; de Freitas Correia, L.N.; (2020). Blue and red light affects morphogenesis and 20-hydroxyecdisone content of *in vitro Pfaffia glomerata* accessions. *Journal of Photochemistry and Photobiology B: Biology*, *203*, 111761.

Shi, H., Chan, Z. (2014). Improvement of plant abiotic stress tolerance through modulation of the polyamine pathway. *Journal of Integrative Plant Biology*, *56*(2), 114–121.

Ramírez-Sánchez, M., Huber, D. J., Vallejos, C. E. (2022). Abiotic stress triggers ROS-mediated programmed cell death in banana (*Musa* sp., AAA group, Cavendish sub-group) fruit. *Scientia Horticulturae*, *293*, 110748.

Shalaby, T A., Taha N A., Taher, D I., Metwaly M., Hossam S. El-Beltagi, Rezk A A., El-Ganainy M S., Shehata W F., El-Ramady H R., Yousry A. Bayoumi A Y. (2022). Paclobutrazol Improves the Quality of Tomato Seedlings to Be Resistant to *Alternaria solani* Blight Disease: Biochemical and Histological Perspectives" *Plants, 11* (3), 425. https://doi.org/10.3390/plants11030425.

Schneider CA, Rasband WS, Eliceiri KW (2012) NIH Image to ImageJ: 25 years of image analysis. *Nature Methods* 9:671–675.

Sahli, M., Rudz, S., Chetehouna, K., Bensaha, R., Korichi, M. (2023). Development, characterization, and photocatalytic study of biocomposites based on PTFE, TiO_2 and *Luffa cylindrica* fibers. *Materials Chemistry and Physics*, *301*, 127635.

Soumya, P. R., Kumar, P., e Pal, M. (2017). Paclobutrazol: a novel plant growth regulator and multi-stress ameliorant. *Indian Journal of Plant Physiology*, *22*, 267–278.

Shahzad, A., Sharma, S., Parveen, S., Saeed, T., Shaheen, A., Akhtar, R., Yadav, V., Upadhyay, A., Ahmad Z. (2017) Historical perspective and basic principles of plant tissue culture. In: Abdin M, Kiran U, Kamaluddin Ali A (eds) *Plant biotechnology: principles and applications*. Springer, Singapore.

Tanimoto, E. (2012). Tall or short? Slender or thick? A plant strategy for regulating elongation growth of roots by low concentrations of gibberellin. *Annals of Botany*, *110*(2), 373-381.

Tanobe, V. O., Sydenstricker, T. H., Munaro, M., Amico, S. C. (2005). A comprehensive characterization of chemically treated Brazilian sponge-gourds (*Luffa cylindrica*). *Polymer Testing*, *24*(4), 474–482.

Tisi, A., Federico R., Moreno S., Lucretti S., Moschou P N., Kalliopi A. Angelakis R, Angelini R., Cona A. (2011). Perturbation of Polyamine Catabolism Can Strongly Affect Root Development and Xylem Differentiation, *Plant Physiology*,*157*(1), 200–215. https://doi.org/10.1104/pp.111.173153.

Tsegaw, T., Hammes, S., Robbertse, J. (2005). Paclobutrazol-induced leaf, stem, and root anatomical modifications in potato. *HortScience*, *40*(5), 1343–1346.

Wen ZZ, Lin Y, Liu YQ, Wang M, Wang YQ, Liu, W (2013) Effects of paclobutrazol *in vitro* on transplanting efficiency and root tip development of *Dendrobium nobile*. *Biologia Plantarum*, *57*(3):576–580.

Waszczak, C., Carmody, M., Kangasjärvi, J., 2018. Reactive oxygen species in plant signaling. *Annual Review of Plant Biology*, *69*, 209–236.

Wang GL, Que F, Xu ZS, Wang F, Xiong AS (2015). Exogenous gibberellin altered morphology, anatomic and transcriptional regulatory networks of hormones in carrot root and shoot. *BMC Plant Biology*, *15*:290.

Yang, Y., Zhang, R., Duan, X., Hu, Z., Shen, M., Leng, P. (2019). Natural cold acclimation of *Ligustrum lucidum* in response to exogenous application of paclobutrazol in Beijing. *Acta Physiologia Plantarum*, *41*, 1-8.

Zhao, J., Lai, H., Bi, C., Zhao, M., Liu, Y., Li, X., Yang, D. (2023). Effects of paclobutrazol application on plant architecture, lodging resistance, photosynthetic characteristics, and peanut yield at different single-seed precise sowing densities. *The Crop Journal*, *11*(1), 301–31.

Zhu, H, Liu J, Wen Q, Chen M, Wang B, Zhang Q, Xue Z (2017) *De novo* sequencing and analysis of the transcriptome during the browning of fresh-cut *Luffa cylindrica* 'Fusi-3' fruits. *Plos One, 12*(11):1–20.

Zhu, L. H., van de Peppel, A., Li, X. Y., Welander, M. (2004). Changes of leaf water potential and endogenous cytokinins in young apple trees treated with or without paclobutrazol under drought conditions. *Scientia Horticulturae*, *99*(2), 133–141.

Ziemmer, JK. (2016) Anatomia do caule de *Merianthera burlemarxii* Wurdack (Melastomataceae). Dissertação (Mestrado em Botânica) - *Setor de Ciências Biológicas*, Universidade Federal do Paraná, Curitiba.

Zhang, M., Li, Q., Liu, T., Liu, L., Shen, D., Zhu, Y., Liu P., Zhou J, M., Dou, D. (2015). Two cytoplasmic effectors of *Phytophthora sojae* regulate plant cell death via interactions with plant catalases. *Plant Physiology*, *167*(1), 164–175.

Figures

Figure 1. Plants of *Luffa cylindrica* grown *in vitro* for 15 days under different concentrations of PBZ. (**a**) 0 – control; (**b**) 0.21 µM; (**c**) 0.42 µM; (**d**) 0.84 µM; (**e**) 1.7 µM; and (**f**) 3.4 µM PBZ. Bar = 6 cm.

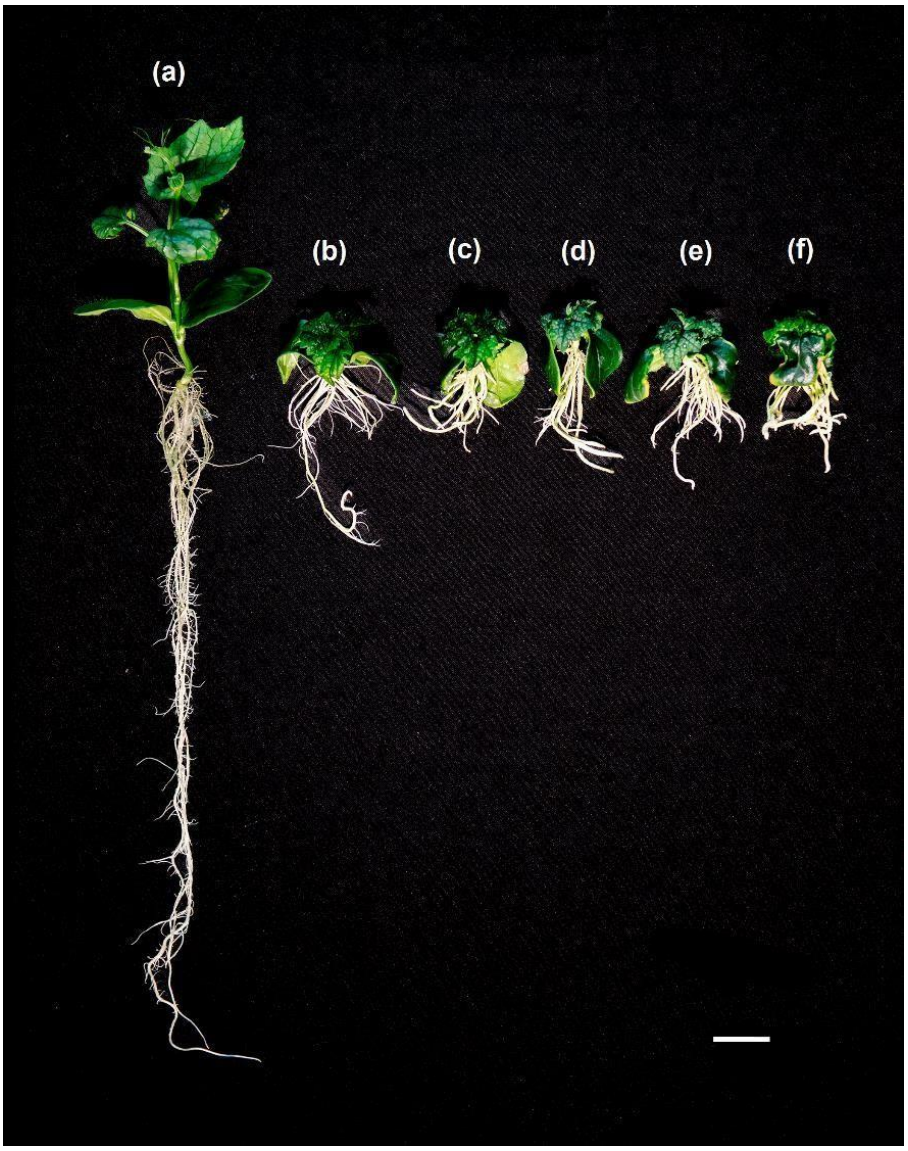

Figure 2. Detail of aerial and root parts of plants of *Luffa cylindrica* grown *in vitro* for 15 days under different concentrations of PBZ. (**a**) 0 – control; (**b**) 0.21 µM ;(**c**) 0.42 µM; (**d**) 0.84 µM; (e) 1.7 µM; and (**f**) 3.4 µM PBZ. Bar = 4 cm.

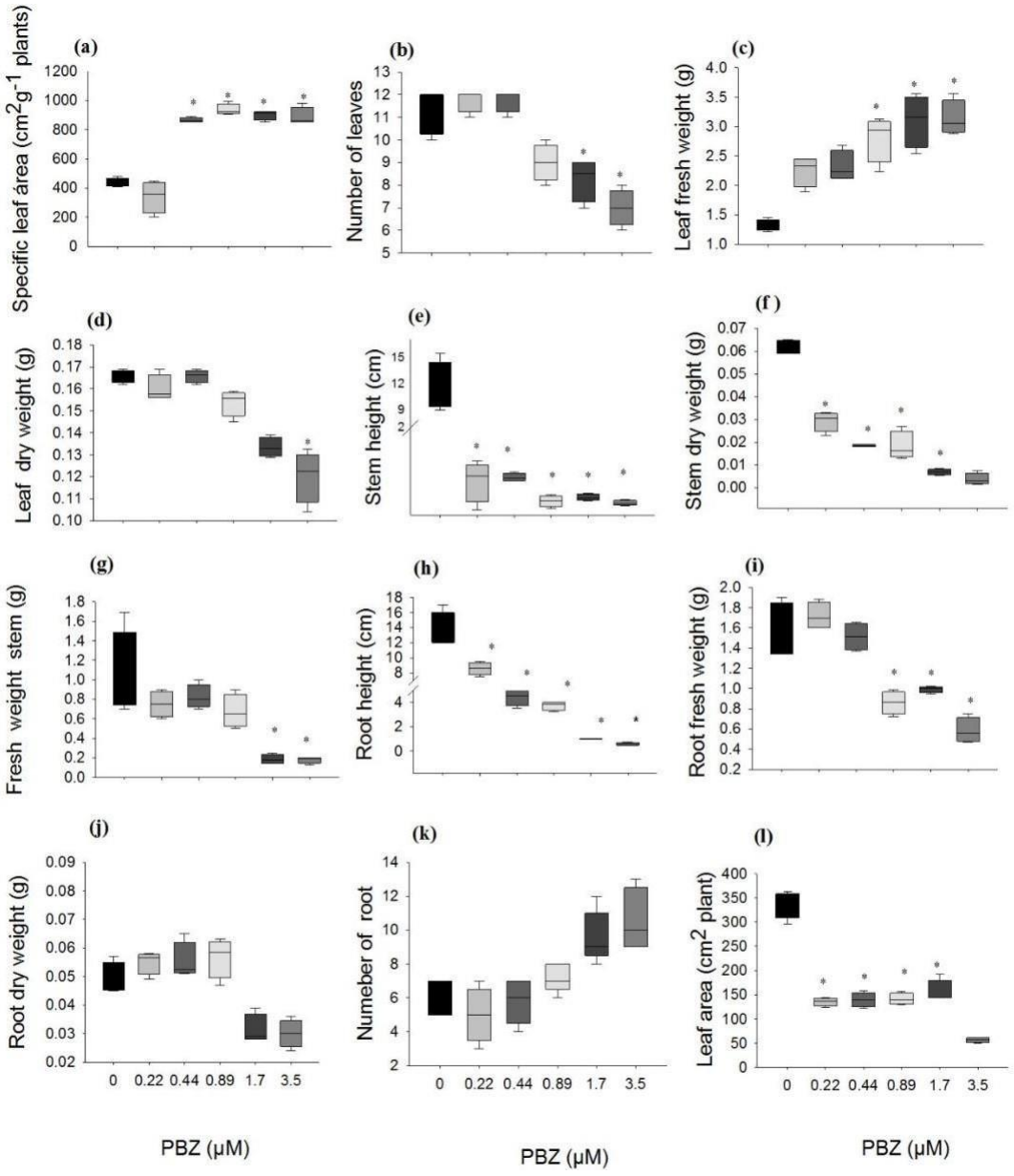

Figure 3. Growth parameters in 15-day-old *Luffa cylindrica* plants exposed *in vitro* to concentrations of Paclobutrazol (PBZ). (**a**) Specific leaf area (cm^2 g^{-1} $plant^{-1}$); (**b**) Left area (cm^2 plant); (c) number of leaves; (**d**) leaf fresh weight (g); (**e**) leaf dry weight (g); (**f**) stem height (cm); (**g**) dry weight stem (g); (**h**) fresh weight stem (g); (**i**) root length (cm); (**j**) root fresh weight (g); (**k**) root dry weight and **(l)** number of roots. Vertical bars represent medians (n = 4). *Asterisks indicate a significant difference at $p < 0.05$ by Dunnett's test.

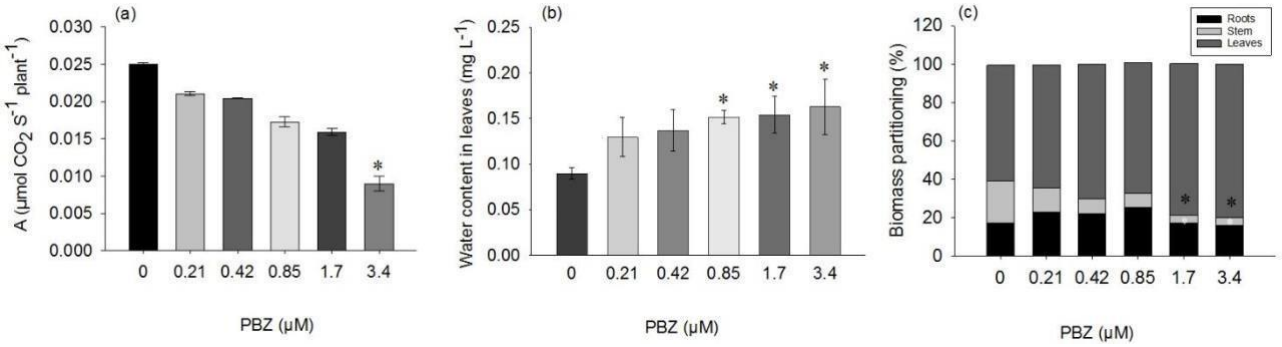

Figure 4. Growth parameters in 15-day-old *Luffa cylindrica* plants exposed *in vitro* to concentrations of Paclobutrazol (PBZ) (**a**) (**a**) Net assimilation rate (*A*); (**b**) Water leaf content (mg L^{-1}); (c) Biomass partitioning (%). Vertical bars represent standard errors of the means (n = 4). *Asterisks indicate a significant difference at $p < 0.05$ by Dunnett's test.

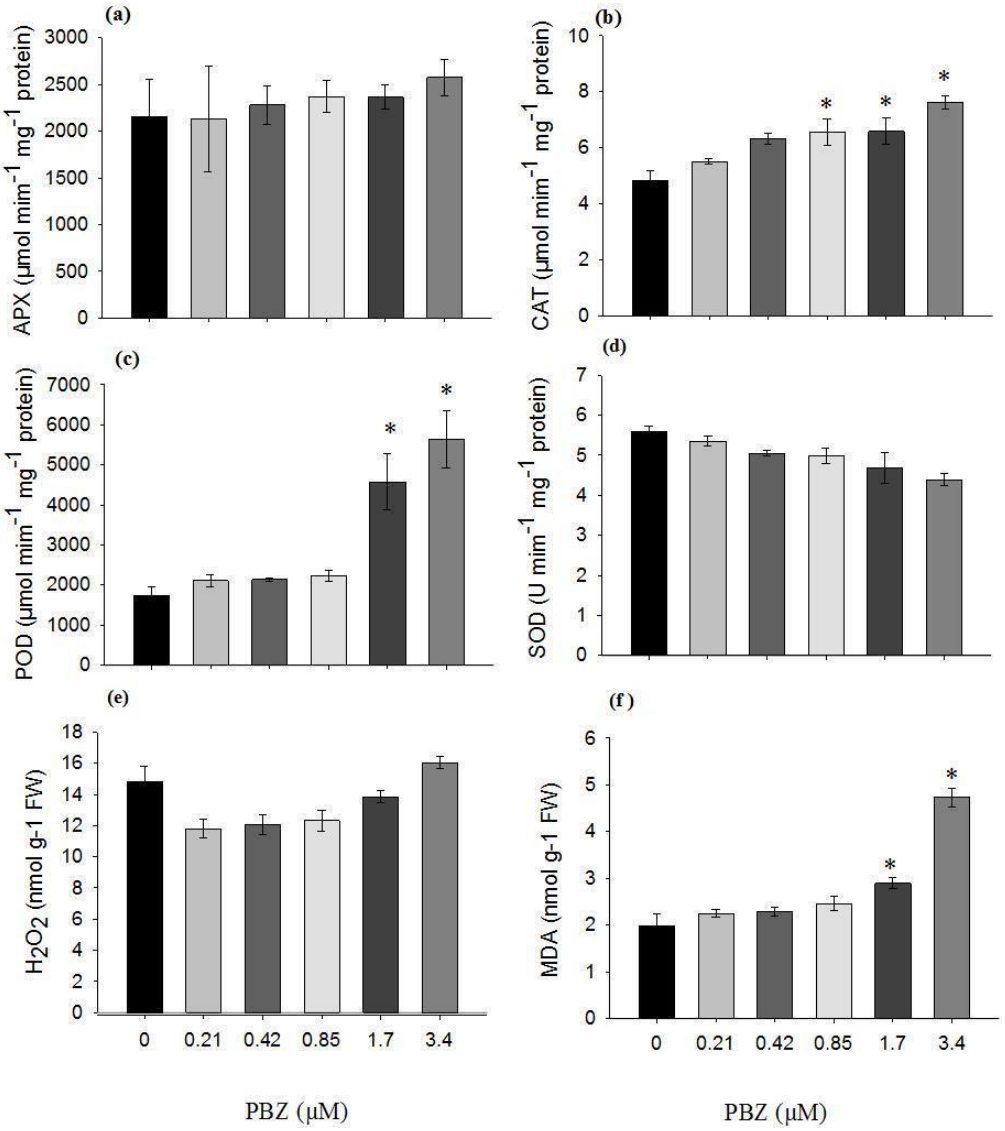

Figure 5. Antioxidant enzymatic activity and lipid peroxidation (MDA content) in 15-day-old *Luffa cylindrica* plants exposed to concentrations of Paclobutrazol (PBZ). (**a**) Ascorbate peroxidase (APX); (**b**) Catalase (CAT); (**c**) Superoxide dismutase (SOD); (**d**) Peroxidase (POD); (**e**) (H_2O_2); (**f**) Malondialdehyde content (MDA). Vertical bars represent standard errors of the means (n = 6), *Asterisks indicate a significant difference at $p < 0.05$ by Dunnett's test.

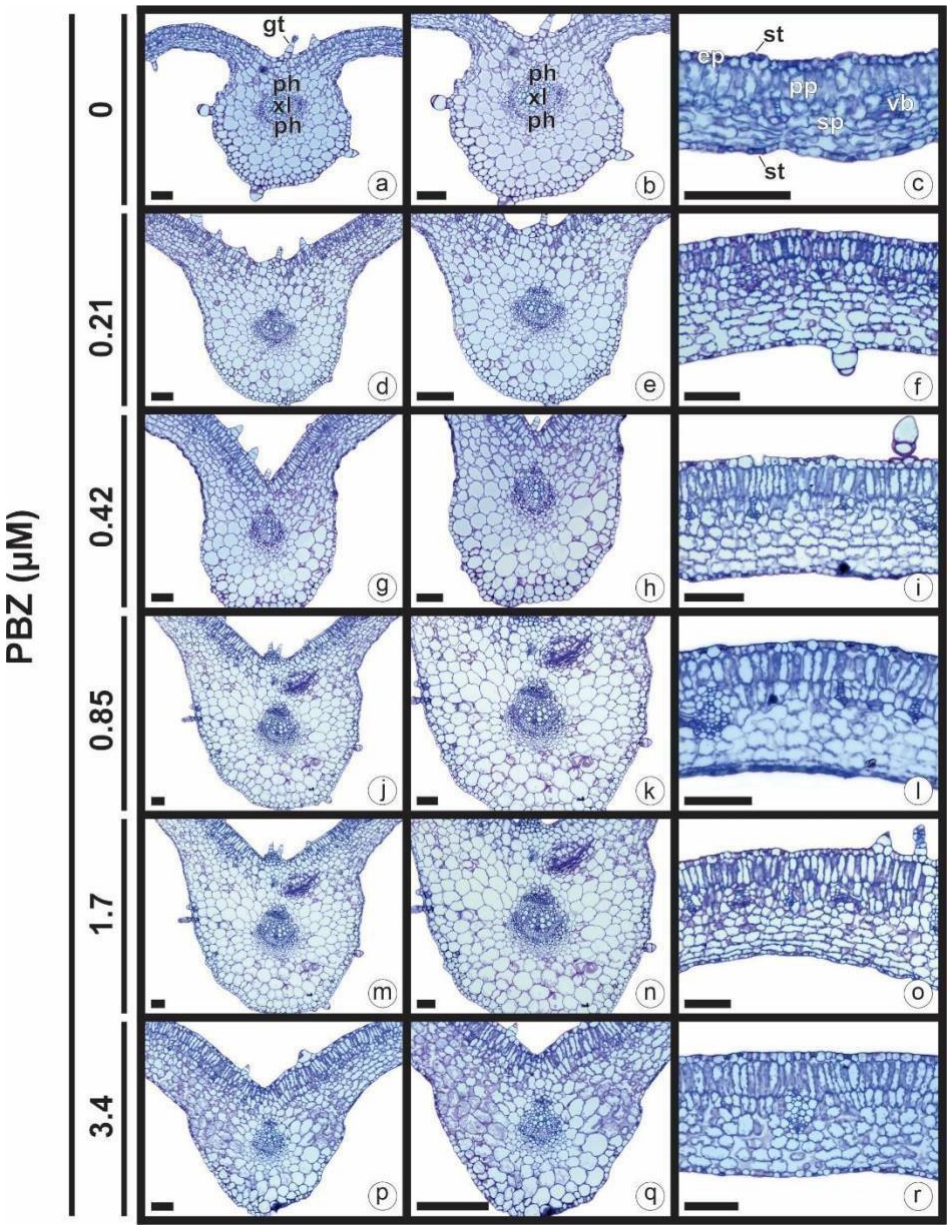

Figure 6. Cross-sections in leaves derived from 15-days-old *Luffa cylindrica* plants exposed *in vitro* to concentrations of Paclobutrazol (PBZ) [0 – control (**a-c**); 0.21 µM (**d-f**); 0.42 µM (**g-i**); 0.85 µM (**j-l**), 1,7 µM (**n-o**) and 3.4 µM (**p-r**). Abbreviations: pp, palisade parenchyma; *sp*, spongy parenchyma; *vb*, vascular bundle; *gp*, ground parenchyma; *gt*, glandular trichome; *co,* collenchyma; *xl*, xylem; *ph*, phloem; *ep*, adaxial epidermis; *ct*, cortex. Bars = 100 µm.

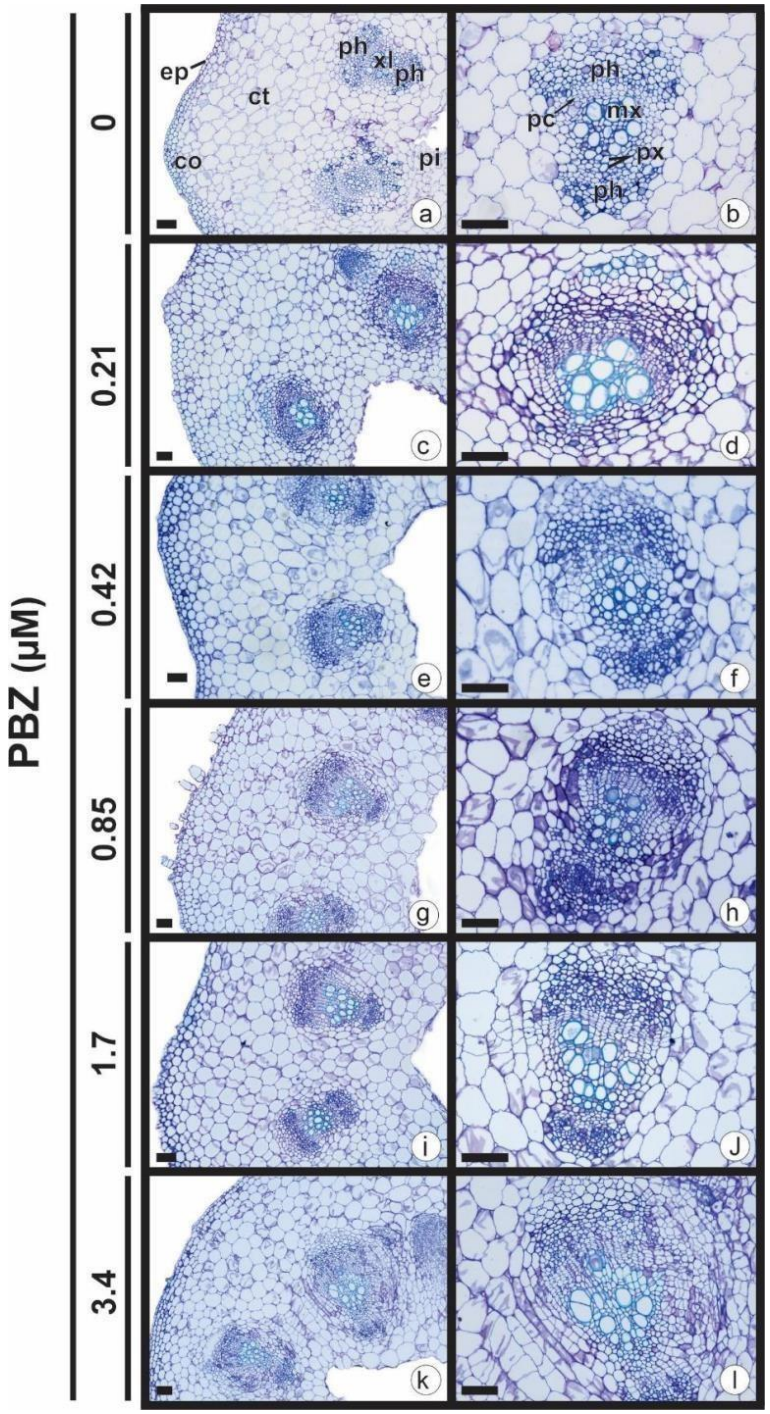
PBZ (µM)
0
0.21
0.42
0.85
1.7
3.4
ep
ct
co
ph
xl
ph
pi
a
ph
pc
mx
px
ph
b
c
d
e
f
g
h
i
J
k
l

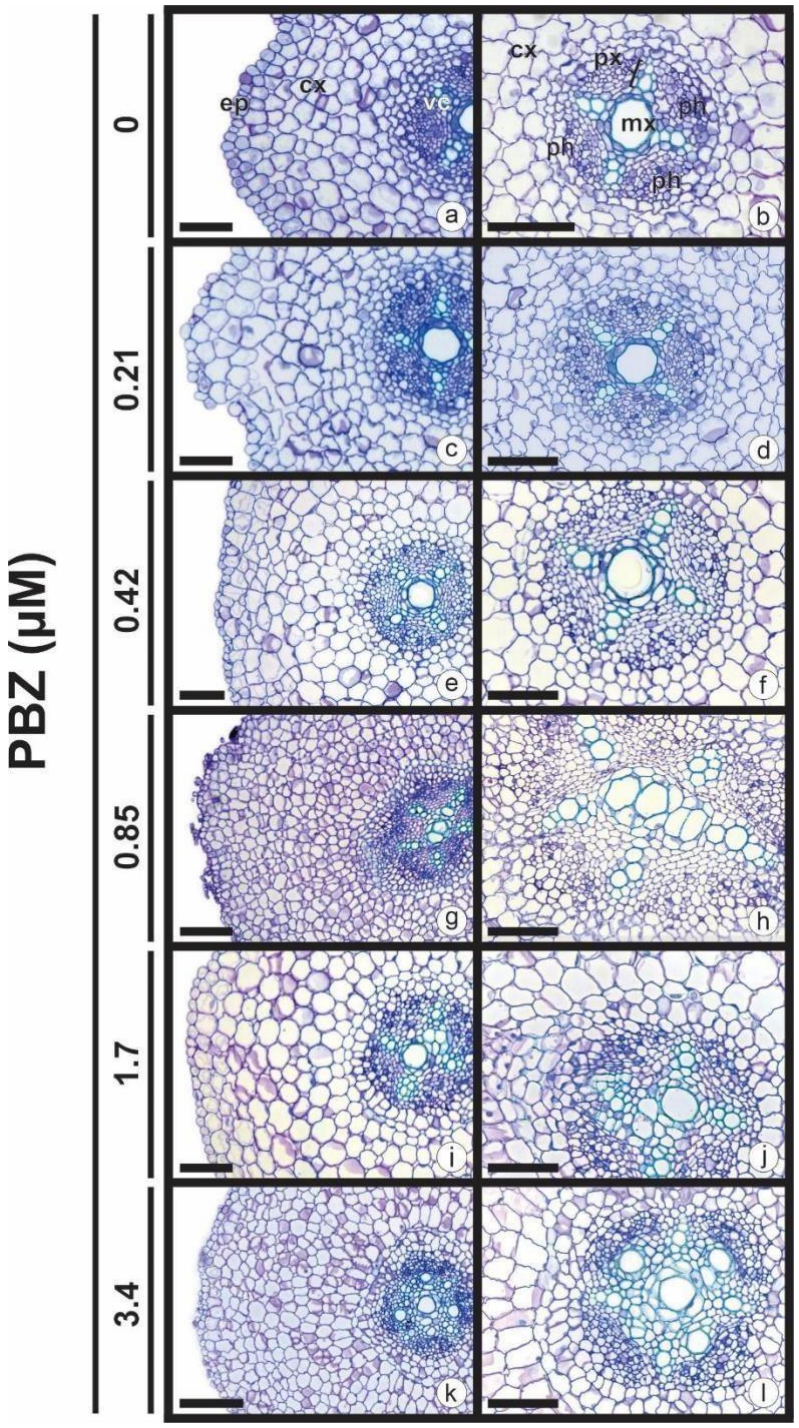

Figure 7. Cross-sections in stem from 15-days-old *Luffa cylindrica* plants exposed to different concentrations of Paclobutrazol (PBZ) [0 – control (**a-b**); 0.21 µM (**c-d**); 0.42 µM (**e-f**); 0.85 µM (**g-h**); 1.7 µM (**i-j**) and 3.4 µM] **(k-l)**. Abbreviations: *ep*, epidermal cells; *ct,* cortex; *vc*, vascular cylinder; *ph*, phloem; *px*, protoxylem; *mx*, metaxylem; *pi*, pith; *pc,* procambium. Bars = 100 µm.

Figure 8. - Cross-sections in roots derived from 15-days-old *Luffa cylindrica* plants exposed *in vitro* to concentrations of Paclobutrazol (PBZ) [0 – control (**a-b**); 0.21 μM (**c-d**); 0.42 μM (**e-f**); 0.85 μM (**g-h**), 1.7 μM (**i-j**) and 3.4 μM] **(k-l)**. Abbreviations: *ep*, epidermal cells; *cx*, cortex; *vc*, vascular cylinder; *ph*, phloem; *px*, protoxylem; *mx*, metaxylem, *pc,* procambium. Bars = 100 μm.

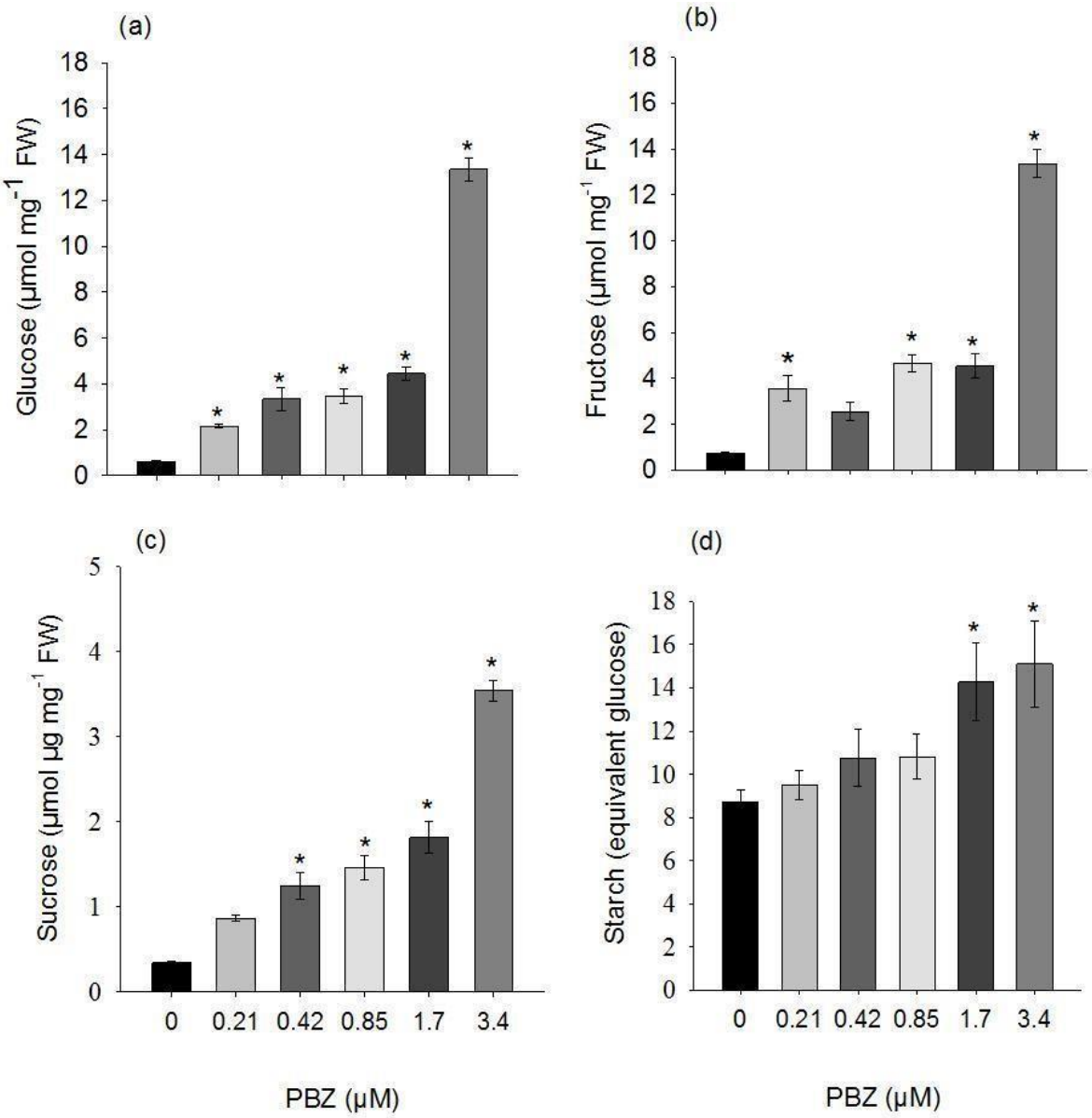

Figure 9. Changes in metabolite contents involved in carbon metabolism in leaf of *Luffa cylindrica* cultivated for 15 days exposed *in vitro* to different concentrations of Paclobutrazol (PBZ). (**a**) Glucose; (**b**) Fructose; (**c**) |Sucrose and (**d**) Starch. Vertical bars represent standard errors of the means (n = 6). *Asterisks indicate a significant difference at $P<0.05$ by Dunnett's test.

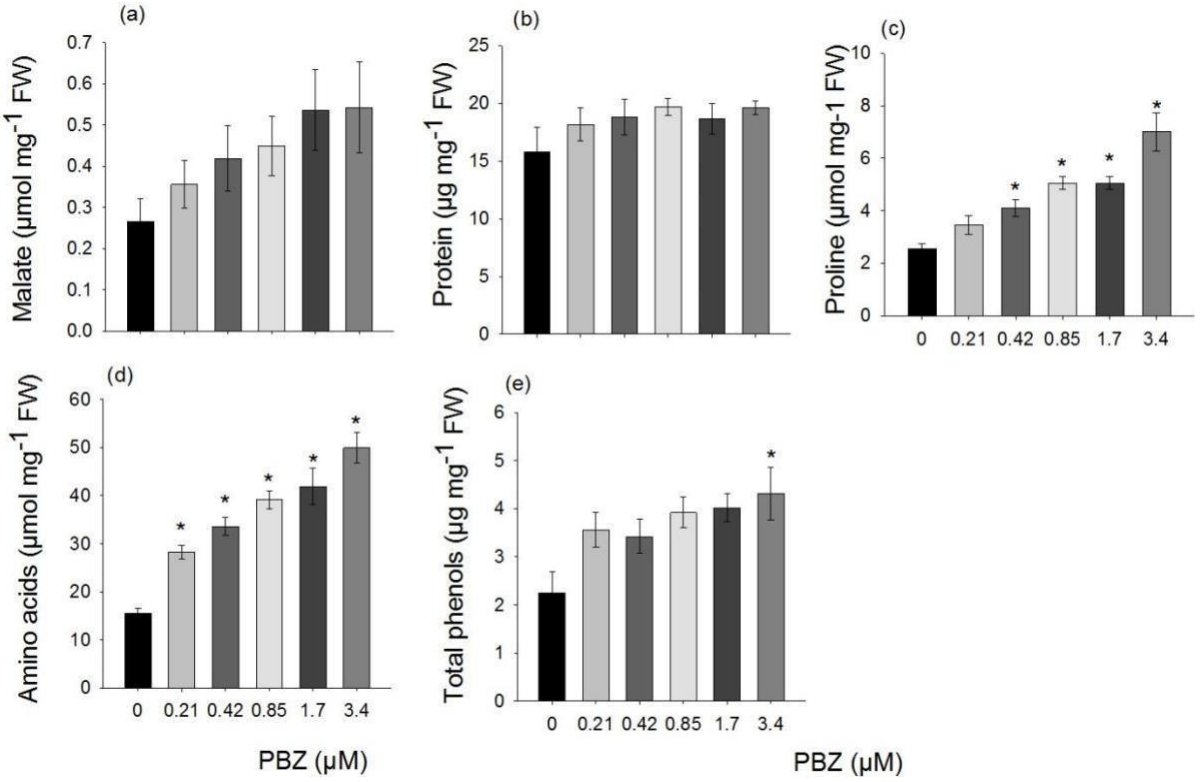

Figure 10. Changes in metabolite contents involved in nitrogen metabolism in leaves of *Luffa cylindrica* cultivated for 15 days exposed *in vitro* to different concentrations of Paclobutrazol (PBZ). (**a**) Malate; (**b**) Protein; (**c**) Proline; (**d**) Amino acids and (**e**) Total phenols. Vertical bars represent standard errors of the means (n = 6). *Asterisks indicate a significant difference at $P<0.05$ by Dunnett's test.

.

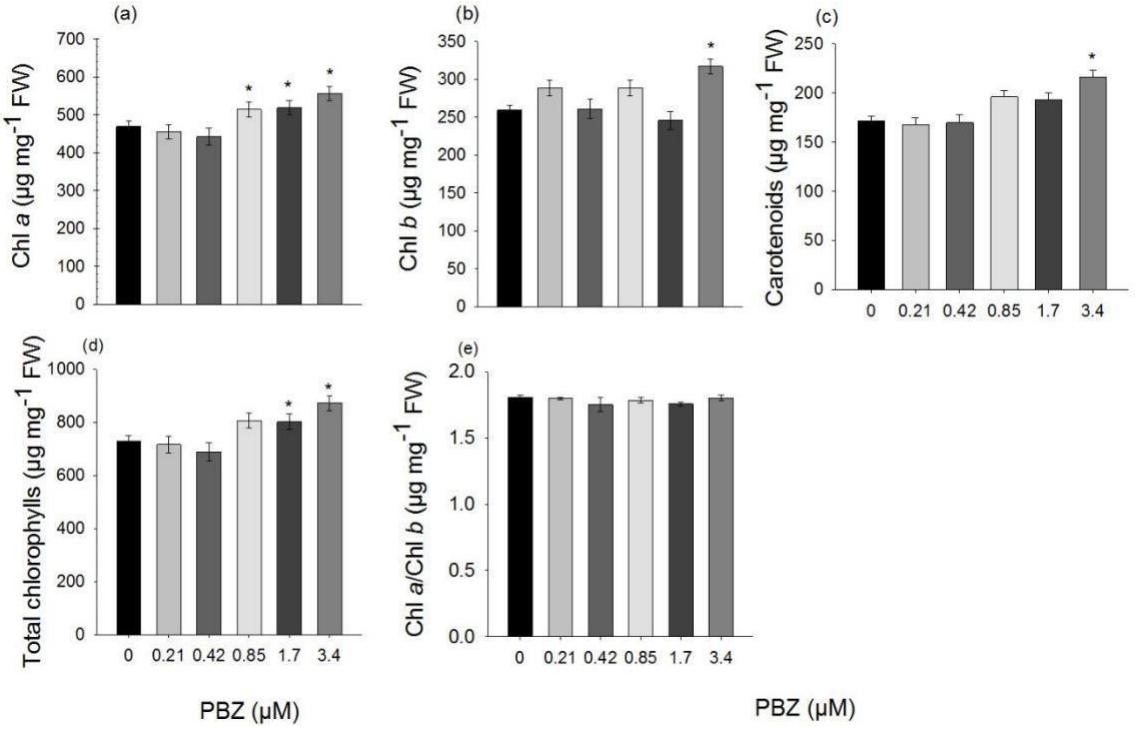

Figure 11. Pigment content in leaves of *L*uffa *cylindrica* plants cultivated for 15 days exposed *in vitro* to different concentrations of Paclobutrazol (PBZ). (**a**) Chlorophyll *a* (Chl *a*); (**b**) Chlorophyll *b* (Chl *b*); (**c**) Carotenoids; (**d**) Total chlorophyll (Chl *a*+Chl *b*); (**E**) Chlorophyll *ab ratio* (Chl *a*/Chl *b*). Vertical bars represent standard errors of the means (n = 6). *Asterisks indicate a significant difference at $P<0.05$ by Dunnett's test.

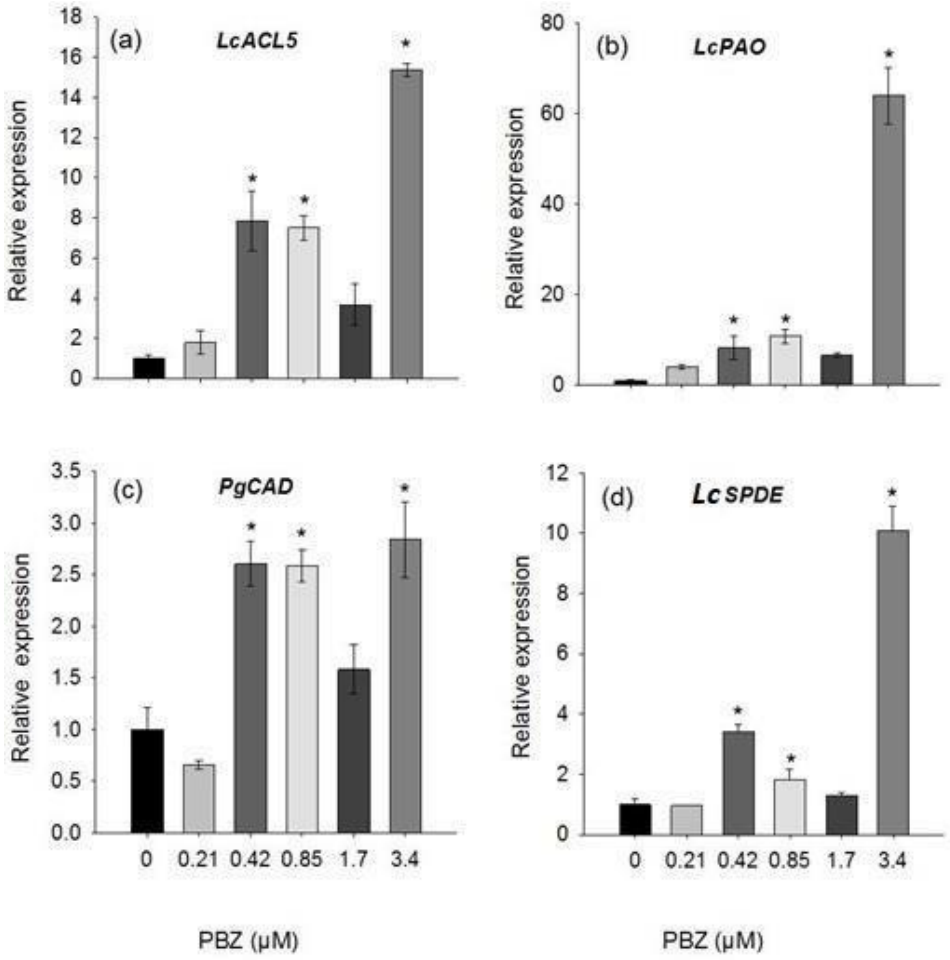

Figure 12. Relative expression of genes from the lignin and polyamine biosynthesis pathway in *Luffa cylindrica* plants at 15 days of growth under Paclobutrazol (PBZ) concentrations. (**a**) *LcACL5*; (**b**) *PgPAO;* (**c**) *PgCAD,* and (**d**) *PgSPDE*. The RPS9 gene normalized expression. Values are presented as means (n=3) ± standard error. *Asterisks indicate significant difference at $p \leq 0.05$ by Dunnett's test.

Tables

Table 1- Morphometric parameters in leaves, root, and stem of *Luffa cylindrica* L. exposed to different concentrations of Paclobutrazol (PBZ) (0 – control, 0.21; 0.42; 0.85, 1.7 and 3.4 µM). Means (n=4) with symbol (*) differ from the standard by $p < 0.05$ by Dunnett's test.

	PBZ (µM)					
	Leaves					
Morphometric parameters	**0**	**0.21**	**0.42**	**0.85**	**1.7**	**3.4**
Vascular bundle size (µm^2)	217.66	184.39	182.56	182.56	176.58	167.35*
Mesophyll size (µm)	219.78	245.89	256.9	268.90*	279.89 *	281.89*
Metaxylem vessel size (µm^2)	20.18	17.18	15.18	15.78	14.67*	13.89*
Length of palisade cells (µm^2)	376.36	428.36	553.60*	546.52	609.30*	614.84*
	Stems					
Vascular bundle size (µm^2)	255.7	324.56	322.67	398.9*	399.98*	425.78*
Cortex size (µm)	339.97	370.66	344.9	334.78	342.76	348.9
	Roots					
Vascular bundle size (µm^2)	420.41	441.87	427.65	468.79	493.45*	641.01*
Cortex size (µm)	119.17	234.67	278.19*	287.95*	290.8*	322.12*

Chapter 2: Investigating the impact of CO_2 enrichment on morphophysiological, biochemical, and molecular characteristics in *Luffa cylindrica* (L.) M. Roem. Plants

Quezia Pains Dutra[1], Tatiane Dulcineia Silva[1], Elisandra da Silva Sousa[1]; Michelle Maylla Viana de Almeida[1]; Auxiliadora Oliveira. Martins[2], Wagner Luis Araújo[2], Wagner Campos Otoni[1].

[1]Department of Plant Biology/Institute of Biotechnology Applied to Agriculture (BIOAGRO), Federal University of Viçosa, 36579-900 Viçosa, MG, Brazil.[2]Plant Growth Unit, Department of Plant Biology, Federal University of Viçosa, 36570-900 Viçosa, MG, Brazil

[2]Plant Growth Unit, Department of Plant Biology, Federal University of Viçosa, 36570-900 Viçosa, MG, Brazil

Abstract

Progressive changes in CO_2 concentration have profoundly impacted plant physiology and phenotypic traits. However, uncertainties persist regarding certain plant responses to elevated CO_2 levels, necessitating further investigation into carbon distribution. This study aimed to explore the effects of elevated CO_2 on morphophysiological, biochemical, and molecular responses in *Luffa cylindrica* L. Plants were exposed to two CO_2 concentrations (± 400 μM mol^{-1} and ± 800 μM mol^{-1}) in open-top chambers (OTCs). Elevated CO_2 significantly increased plant height and root length, alongside an increase in dry and fresh mass, biomass, and specific leaf area over time. Enzyme activity (CAT, SOD, POD, APX) remained unchanged, while sugar content increased after 25 days under high CO_2. Elevated CO_2 led to increased carbohydrate levels, supporting the biosynthesis of vital compounds for plant growth and development. Additionally, upregulation of genes involved in lignin and polyamine biosynthesis pathways was observed. These findings highlight the photosynthetic efficiency under high CO_2 concentrations, promoting plant growth and development. The study underscores the species' adaptive efficiency and metabolic reorganization in response to future high CO_2 environments, offering insights into the broader implications of climate change on agricultural adaptations, biodiversity conservation, and human health.

Key-words: Climate change; CO_2 enrichment; growth; morphophysiology; metabolism; sponge-gourd.

Introduction

Climate change is a challenge for crop development. These changes are occurring partly due to human action, the use of fossil fuels, deforestation, among others. CO_2 levels have been increasing significantly over the years and changes in temperature and precipitation are observed (Soares et al., 2019). The impacts of this are observed in the productivity of plants in their photosynthetic metabolism and biosynthesis of compounds (Salihi et al., 2023).

The increase in carbon dioxide (CO_2) concentration in the atmosphere is not an isolated climatic condition in the context of the global warming phenomenon. Extreme climatic events, such as periods of drought, intense heat, frost, or the interaction of these stresses, are intrinsically linked to the impacts resulting from the increase in CO_2, exerting diverse influences on the production of primary and secondary metabolites in plants (Ahmed et al., 2019; Birami et al., 2020). To gain a deeper understanding of plants' physiological and metabolic responses to climate change, it is advisable to use techniques such as CO_2 enrichment under field conditions (FACE) or in controlled environments such as open-top chambers (OTC).

Studies have shown that plants under stress conditions and with high CO_2 availability can optimize the net photosynthetic rate, increasing hexoses, promoting an accumulation of starch, citric acid and others (Li et al., 2022; Salihi et al., 2023; Zhang et al., 2023). In grains, e[CO_2] can decrease the levels of proteins, Mg, Fe and Zn (Ebi et al., 2021). This is due to "carbohydrate dilution", as the carbon-nitrogen ratio and reduced transpiration reduce mass flow and nutrient reallocation for biochemical processes (Matimati et al., 2014; Soares et al., 2019). However, e[CO_2] can increase the concentration of proteins, carbohydrates, phenols, and others. This favors the translocation of photoassimilates, contributing to growth and development. In *Zingiber officinale*, it was observed that high CO_2 concentrations favor the synthesis of primary metabolites, antioxidant enzymes and increased biomass (Ghasemzadeh and Jaafar, 2011). In melons, it has been observed that CO_2 enrichment increases photosynthetic enzymes and fruit quality and production (Han et al., 2023). However, more research is needed to understand the impacts of a CO_2-enriched atmosphere. *Luffa cylindrica* L. is an annual herbaceous species belonging to the Cucurbitaceae family. It is popularly known as ‘bucha’, ‘esfregão’, ‘esponja vegetal’, ‘bucha dos paulistas’, ‘pepino bravo’, ‘gonçalinho’, ‘maxixe do Pará’, among others. Native to Asia, it was introduced to Brazil by the Portuguese and is currently

cultivated throughout Brazil, especially in the state of Minas Gerais (Marouelli et al., 2013; Barroso et al., 2014; Chen et al., 2015). This species is of economic importance mainly due to its fruits, which are used in folk medicine to make handicrafts and industrial products and for aesthetic purposes (Du et al., 2006; Partap et al., 2012). The fruit of the bush is cylindrical, slightly angular and bent, with a variation in size (Laidani et al., 2012). In the process of ripening, the fruit is made up of a tangle of multidirectionally arranged fibers composed mainly of cellulose, hemicellulose and lignin, and is therefore called lignocellulosic (Tanobe et al., 2005). The event of programmed cell death gives them their fibrous appearance, which thickens the secondary wall and accumulates lignin in the parenchyma cells (Zhu et al., 2017).

In this scenario, we propose a hypothesis: the growth of *L. cylindrica* under high CO_2 conditions may result in increased biomass and alterations in its composition, potentially enhancing crop yields. This investigation aims to shed light on the adaptation strategies employed by plants in response to these conditions.

Materials and Methods

Plant material and experimental design

Mature seeds of *Luffa cylindrica* purchased from Feltrin Sementes (Farroupilha, RS, Brazil) were mechanically scarified to remove the aryl. Seeds were then immersed in 70% (v/v) ethanol for 1 min, transferred to a 2.5% (v/v) solution of sodium hypochlorite containing 0.1% (v/v) of Tween 20 for 20 min. Then, seeds were washed in sterile distilled water (autoclaved at 120 ºC and 108 kPa for 20 min).

The seeds were then inoculated into Petri dishes containing 20 mL of half-strength MS-based medium (Murashige and Skoog, 1962) supplemented with 50 mg L^{-1} myo-inositol, 1.5% sucrose (w/v) and 6.5 g L^{-1} agar (PhytoTechnology Laboratories®, Overland Park, KS, USA). The pH of the medium was adjusted to 5.7 ± 0.01, followed by autoclaving at 120 °C and 108 kPa for 20 min. The cultures were kept in a growth room at 25 ± 2 °C under a photoperiod of 16 h of light, under an irradiance of 60 μM m^{-2} s^{-1} with two LED lamps (SMD 100, 18 W, Vilux®, Vitória, ES, Brazil), where they remained until the radicle emerged, about three days.

After the rootlets emerged, they were transplanted into plastic pots with 3 kg of Tropstrato HT® commercial substrate (Vida Verde, Mogi Mirim, Brazil) and placed in open-top chambers (OTC) (1.15 m in diameter and 1.40 m high) and subjected to a CO_2-enriched atmosphere. CO_2 fumigation was carried out from 06:00 to 18:00 and [CO_2], temperature, and humidity were checked daily using portable CO_2 sensors (model CO277, Akso Produtos Eletrônicos, São Leopoldo, Brazil). During cultivation in the greenhouse (25-day experiment), the plants were fertilized on days 1 and 15 with 5.5 g of NPK - 15:09:12 (Osmocote® Plus, São Paulo, Brazil).

The experiment was designed in a completely randomized scheme, corresponding to two CO_2 concentration regimes: ambient [CO_2] (a[CO_2], ≈400 μmol mol^{-1}); and elevated [CO_2] (e[CO_2], ≈800 μmol mol^{-1}). After 15, 20, and 25 days of experiment in OTC, collections were made. The parameters evaluated were growth and leaf area. Leaf, stem and root sections were collected for anatomical characterization. In addition, leaf samples were collected and frozen in liquid nitrogen and stored at -80° C for subsequent biochemical and molecular analysis.

Growrh parameters

Stem length (cm), number of branches, dry mass (g), number of leaves, and leaf area (cm^2) were measured. To determine leaf area, leaves were detached and fixed individually on white plasticized graph paper. Photographs were taken with a digital camera and images were processed using ImageJ software (Schneider et al., 2012). Dry weight (g) was obtained by oven-drying the plant material at 50 °C for 72 h.

Antioxidant activity

Activity of oxidative stress enzymes, superoxide dismutase (SOD), catalase (CAT), peroxidase (POD), and ascorbate peroxidase (APX) was assessed. Briefly, 50 mg of frozen fresh material (leaf) were homogenized in 1 mL extraction medium containing 0.1 M potassium phosphate buffer, pH 6.8; 0.1 mM ethylenediaminetetraacetic acid; 1 mM phenylmethylsulfonyl fuoride and 1% (w/v) polyvinylpolypyrrolidone (PVPP). The samples were vortexed for 10 s, centrifuged at 12,000 rpm for 15 min at 4ºC, and the supernatant was removed and set aside on ice for enzyme assays plus protein determination (Bradford, 1976). CAT, APX, and POD activities were determined as proposed previously (Chance and Maehly, 1955; Nakano and Asada, 1981; Havir and McHale, 1987) and expressed as μM^{-1} min^{-1} g^{-1} protein. SOD activity was measured as described earlier (Giannopolitis and Ries, 1977) and expressed as U min^{-1} g^{-1} protein, with 1 U being equivalent to the concentration of SOD required to inhibit 50% of nitro blue tetrazolium photoreduction.

Determination of lipid peroxidation

Lipid peroxidation was indirectly estimated by determining the malonaldehyde (MDA) content according to the methodology described previously (Lima et al., 2002). Aliquots of approximately 100 mg of fresh leaf mass were used for this analysis. The samples were extracted with trichloroacetic acid (TCA). 1 mL of 1% (w/v) TCA was added to the 1.5 mL microtubes containing the macerated material, homogenized, and centrifuged for 15 min at 10,000 x *g* at 4°C. The supernatant fraction was transferred to another microtube. This process was carried out twice; the supernatants, mixed in the

same microtube, was quantified, and the precipitate discarded. MDA quantification took place after adding 750 µL of 20% TCA with 0.5% thiobarbituric acid (TBA) to a screw cap microtube already containing a 500 µL aliquot of the extract. The tubes were incubated for 30 min at 95 °C with gentle agitation and after this period, the reaction was stopped in an ice bath. In a microplate, 300 µL of each sample were added in triplicate. Readings were taken at two wavelengths, 532 and 600 nm. Once the absorbance values were obtained, the averages of the triplicates were taken, and the MDA concentration was determined using the equation from (Heath e Packer 1968), expressing the results in nmol g^{-1} FW.

$$\text{MDA (nmol mL}^{-1}) = \frac{(A_{532} - A_{600}) * 10^6}{155000}$$

Metabolites analysis

Leaf samples (second fully expanded leaf from the apex of the plants) were collected at 12:00 pm (noon). The samples were frozen in liquid nitrogen and subsequently ground for analysis. About 25 mg of freeze-dried tissues were used for extraction with methanol as described and adapted by Lisec et al., (2006). Photosynthetic pigments were determined as described Wellburn (1994). Carbohydrates (starch, sucrose, glucose, and fructose) were assessed as described by Fernie et al. (2001). Soluble total protein was assessed as described by Bradford, (1976) and total amino acid contents were analyzed according to Yemn and Cocking, (1995). Proline content followed the methodology proposed by Carillo e Gibon, (2011). Five replicates were used for each treatment.

Anatomical characterization

For the anatomical studies, transverse sections of leaves, stems and roots were collected at different times (15, 20 and 25 days). The samples were then fixed in 4% glutaraldehyde solution. After fixation, the samples were dehydrated in ethanolic series and embedded in acrylic resin (Historesin®, Leica Instruments, Wetzlar, Germany). Transverse sections (5-µm-thick) were obtained on an automatic feed rotary microtome (RM2155, Leica Microsystems Inc., Buffalo Grove, IL, USA). For structural

characterization, samples were stained with toluidine blue (pH 3.2) for 3 min (O'Brien and McCully, 1981). The sections were then mounted on glass slides with Permount® SP15-500 synthetic resin (Fisher Chemicals, Thermo Fisher Scientifc, Waltham, MA, USA) and observed under a light microscope.

RNA extraction, cDNA synthesis, and quantitative PCR analysis

Total RNA was extracted from leaf samples using TRI Reagent® (Sigma-Aldrich Co.), as recommended by the manufacturer. The cDNA was then synthesized using the Superscript™ III kit (Invitrogen, Carlsbad, CA, USA). We evaluated the expression of the gene belonging to the lignin biosynthesis pathway: *Cinnamyl alcohol dehydrogenase* (*PgCAD*) and *Cafeato o-methyltransferase* (*PgCOMT*) (Batista et al., 2019) and genes designed based on the *Luffa cylindrica* transcript: *Thermospermine synthase* (*LcACL5*). The *40S ribosomal protein S9* gene (*BoRPS9*) was used for normalization (Moreira et al., 2018). Expression analyses were performed by real-time PCR on a CFX96 Touch™ device (BIO-RAD) using SYBR Green Master Mix (BIO-RAD). The reactions were performed with four biological replicates each in duplicate technique, in a reaction volume of 10 µL (4 µL of SYBR-Green, 0.2 µL of each primer, 3.6 µL of diethylpyrocarbonate-treated water and 2 µL (40 ng) of cDNA. The amplification conditions were carried out in the following steps: 2 min at 50 ºC and 10 min at 95 ºC, followed by 40 cycles of 95 ºC for 15 s and 60 ºC for 60 s, and the dissociation curve from 60 to 95 ºC at 0.5 ºC s^{-1}. Transcription levels were determined using the $2^{-\Delta\Delta Ct}$ method (Livak and Schmittgen, 2001), with three biological replicates with at least two technical replicates each.

Results

Elevated CO_2 promoted greater biomass accumulation

After 25 days of cultivation in the OTCs, the growth and development of *L. cylindrica* L. were significantly different (Figs. 1 and 2). Compared to a[CO_2], e[CO_2] significantly increased specific leaf area at 20 and 25 days of the experiment (Fig. 3d), this increase exceeds 100% to 25 days. Similar to what was observed in SLA, large increases were also observed for dry biomass of leaves and roots (Figs. 3c and j) and fresh weigth of stem (Fig. 3f). The other parameters showed a significant increase at 25 days in e[CO_2] when compared to the control, although in the other times we can observe a tendency of increase. Although the number of leaves did not differ between treatments (Fig.3a), it is noteworthy that plants under high CO_2 show a large investment in leaf biomass to the detriment of the stem (Fig. 3k). It is noteworthy that this remobilization of biomass did not affect the root system.

Elevated CO_2 promoted anatomical changes

The expanding leaves are made up of juxtaposed cells with a dense nucleus, uniseriate epidermis with the presence of trichomes, a large central vascular bundle with parenchyma distributed along the main vein. Also observed was a subepidermal collenchyma on the adaxial surface and the leaf blade subdivided into palisade expanding leaves and mature leaves of plants grown in different [CO_2] conditions for 15 days (Figs. 7a, d, g and j). At 20 days the palisade parenchyma of the mesophyll was composed of two layers in the control and elongated in high CO_2 (Figs. 8a, d, g and j). At 25 days, the presence of apparently shortened spongy parenchyma under conditions of high CO_2 (Fig. 9a, d, g and j).

The stems of both conditions, at 15 days, have a defined vascular system, well-defined cambial cells, and the beginning of fiber formation (Figs. 7b, e, h, and k). After 20 days, the epidermis is uniseriate with subepidermal collenchyma and a cord of fibers above the vascular system (Figs. 8b, e, h and k). Secondary growth was represented by the vascular cambium, which predominantly produces xylem (Figs. 9b, e, h and k).

For the root, at the 15 days, the cortex was more widely spaced in control compared to the high CO_2 condition, which showed fewer cells (Figs. 7c, f, i and l). At 20 days, fibers were present in both conditions (Figs. 8c, f, i and l). At 25 days, secondary phloem and rays were present in both treatments (Figs. 9c, f, i and l), displaying a well-defined and elongated vessel element.

Primary metabolism is altered by elevated CO_2

When evaluating pigment content in leaves of *L. cylindrica*, we observed an opposite behavior between the different CO_2 concentrations, although this behavior was not significant (Fig. 5). In a [CO_2] the pigments increased over time, while in e[CO_2] there was a reduction. However, only after 25 days were there significant reductions in Chl*a* (Fig. 5a) and Chla+b (Fig. 5c). To Chl*b* and carotenoids, showed no significant differences between the control and the times (Figs. 5b and d). No specific pattern was observed between treatments in relation to the metabolite's glucose, fructose, sucrose, starch, amino acids and total proteins. Only after 15 days of treatment was there a 1-2-fold increase in soluble sugars in e [CO2] when compared to the control (Figs. 6a, band c), the same was found to starch and soluble total proteins (Figs. 6e and f). It is noteworthy that the starch content increased over time, but without differing between treatments at 20 and 25 days.In the presence of e[CO_2], the amino acids content showed a significant 1.5-fold increase after 20 days compared to the control (Fig. 6d), while on the other evaluation days this content was reduced. For proline, an amino acid involved in membrane protection, there was a significant decline at 15 days of experiment for e[CO_2] compared to the control and remained low over time, which was also verified in the control condition (Fig. 6g). As for phenolic compounds, there was an increase over time for the control condition, while in e[CO_2] there were reductions, this being significant at 25 days (Fig. 6h).

Antioxidant enzymes and MDA content are not affected by high CO_2

In general, the increase in atmospheric CO2 did not result in the generation of oxidative stress in the on *L. cylindrica* plants. The activity of the antioxidant enzymes CAT, SOD, APX and POD (Figs. 4b, c, d and e, respectively)) and the MDA content (Fig. 4f) were not significantly influenced by [CO_2]. CAT activity did not show a tendency to increase over time as was observed for the other enzymes between 15 and 20 days of

cultivation. The tendency of reduction on MDA contents in the MDA content over time and in the presence of high CO_2 (Fig. 4f) corroborates the reduced H_2O_2 data verified in the presence of CO_2 enrichment at 20 and 25 days (Fig. 4a).

Elevated CO_2 modulated the expression of genes related to the lignin and polyamine biosynthetic pathway.

In the phenylpropanoid biosynthesis pathway, the expression of lignin-related genes, *PgCOMT, was* positively influenced by e[CO_2]. Compared to a[CO_2], *PgCOMT* increased 2.8-fold in plants under e[CO_2] (Fig. 10c). In the polyamine biosynthesis pathway, the expression of the *LcACL5* gene showed a 2-fold increase when compared to the control (Fig. 10b). The *PgCAD* gene showed no significant difference in its expression level (Fig. 10a).

Discussion

It is widely believed that increased atmospheric CO_2 aids in plant growth and development, as this higher amount can provide plants with sugars as an energy source (Takatani et al., 2014). The present study demonstrates an increase in stem length, root number, and both fresh and dry mass after 20 and 25 days under elevated CO_2 conditions. This enhancement is attributed to increased vigor, as observed initially under elevated CO_2 conditions. These findings are consistent with those of Yu et al. (2017) for the species *Cynodon dactylon* and Saha et al. (2013) for chickpeas, both of which showed increased plant height and stem length, as well as a decrease in chlorophyll content under elevated CO_2 conditions.

This study showed us that plants in e[CO_2] can develop and have survival strategies. A strong root system is the key to increasing productivity (Malamy, 2005). The well-developed epidermal structure of the roots facilitates interaction with the soil environment, favoring the absorption of water and nutrients (Malamy, 2010; Cassan et al., 2023). This can be seen in the increase in root length, fresh and dry mass after 25 days of experimentation. In studies carried out by He et al. (2016), e[CO_2] promoted an increase in the size of lettuce roots and thus altered their metabolism due to the availability of substrate for the biosynthesis of compounds (Gao et al., 2022).

Plants need a quantity of carbon to build up molecules that perform various functions, such as providing energy. At high CO_2 concentrations, the amount of carbon can increase and consequently activate photosynthetic pathways. In addition, it can activate the biosynthesis of metabolism compounds, helping plant growth and development (Du et al., 2014; Li et al., 2020). According to Reddy et al. (1998), CO_2 enrichment aids the expansive growth of leaves, increasing their leaf area and dry mass. In *Phaseolus vulgaris*, leaf area and volume increased due to growth in the density of epidermal cells and mesophyll (Bray and Reid, 2002). Another important point is that carbohydrates may be redirected to the formation of mitochondria, providing more energy for biosynthetic processes and respiratory capacity (Li et al., 2013).

This study observed biochemical changes, such as a decrease in H_2O_2. The other enzymes showed no significant differences. This may be due to the plants' ability to resist intrinsic oxidative damage (Hongxu et al., 2001). Furthermore, as the plants were not subjected to stress, there is no need for energy expenditure (Yu et al., 2004). The increase in CO_2 increases the availability of sugars that are directed towards growth and

development. According to Pritchard et al. (2000), soybean plants subjected to e[CO_2] decreased the activity of stress enzymes, chlorophylls, carotenoids, and soluble proteins.

The activities of glucose, fructose and sucrose increased in 15 days of cultivation and after 20 days, however without significant differences in e[CO_2]. This shows that e[CO_2], combined with the increase in these sugars, drove faster growth. In response to the increase in sugar synthesis, there is an accumulation of starch. This can be seen in the present work and studies by Larios and collaborators (2004). Research on the Cucurbitaceae family has shown that some representatives respond positively to e[CO_2]. This is related to the ability to translocate photoassimilates, the source-drain relationship (Agüera et al., 2006; Song et al., 2020). Another important point is that the accumulation of starch can affect the rate of CO_2 assimilation, hindering its diffusion, and can undergo photosynthetic acclimatization under e[CO_2] in the long term (Nafziger and Koller, 1976; Li et al., 2022). According to Ainsworth and Bush (2011) and Blaschke et al. (2011), high levels of CO_2 increase investment in its metabolism, so it accumulates sugars that help to maximize photosynthesis and production. In addition, compounds that are important for growth and development, such as lignin, can accumulate. This study showed an increase in the expression of *LcACL5* and *PgCOMT*, which are responsible for the biosynthesis of polyamines and lignin. This suggests a greater development of vessel elements and the formation of secondary walls and, consequently, greater cell lignification. We believe that in plants grown under e[CO_2], biomass accumulation and photosynthesis may be related to the higher lignin content. In studies carried out by Niinemets et al. (2011), it was shown that at high CO_2 the plants showed a decrease in leaf lamina, epidermis and palisade parenchyma and thick wall. This may be due to an increase in intercellular spaces and consequently an increase in mesophyll conductance to CO_2 and lignin accumulation (Bahamonde et al., 2023). Therefore, growing *L. cylindrica* plants in e[CO_2] may represent a strategy for obtaining plants with greater biomass and altering the content of compounds that aid their growth and development. Thus, it could open up possibilities and contribute to elucidating the morphophysiological, biochemical and molecular responses of *Luffa* to climate change, especially in relation to e[CO_2].

Conclusion

This comprehensive study elucidated the multifaceted effects of PBZ on the morphophysiological responses of *L. cylindrica* grown *in vitro*. The results revealed a

combined impact on various aspects of plant development, underlining the problematic interaction between PBZ and plant physiology. PBZ significantly influenced leaf growth dynamics, and noteworthy morpho-anatomical changes were also observed, including a more pronounced vascular system with greater xylem differentiation and an increase in the cortex. These changes reflect the results of other studies, indicating a consistent impact of PBZ on plant anatomy. In addition, this study elucidated the biochemical changes induced by PBZ, revealing its ability to disrupt hormonal balance, particularly affecting GA, ABA, ethylene and cytokinins. This hormonal disruption led to inhibition of cell elongation, as evidenced by reduced growth and smaller cell diameter. These effects were consistent with previous observations in various plant species, affirming the far-reaching influence of PBZ on growth regulation. Finally, this research contributes valuable information on the diverse and intricate effects of PBZ on the morphophysiological aspects of *L. cylindrica*, highlighting the need for a comprehensive understanding of the complex interactions between plant growth regulators and plant physiology for sustainable and effective agricultural practices.

References

Agüera, E., Ruano, D., Cabello, P., Haba, D. L. P. (2006). Impact of atmospheric CO_2 on growth, photosynthesis and nitrogen metabolism in cucumber (*Cucumis sativus* L.) plants. *Journal of Plant Physiology*, *163*(8), 809–817.

Ahammed, G. J., Li, X., Liu, A., Chen, S. (2020). Physiological and defense responses of tea plants to elevated CO_2: A Review. *Frontiers in Plant Science*, *11*, 305 https://doi.org/10.3389/fpls.2020.00305.

Ayvaci, U., Koc, F. N., Cetinkaya, H., Seckin Dinler, B. (2023). Treatment with auxin and paclobutrazol mediates ROS regulation, antioxidant defence system and cell wall response in salt treated soybean. *Brazilian Journal of Botany* https://doi.org/10.1007/s40415-023-00922-8.

Bray, S, Reid, D. M. (2002). The effect of salinity and CO_2 enrichment on the growth and anatomy of the second trifoliate leaf of *Phaseolus vulgaris*. *Canadian Journal of Botany*, *80*(4), 349–359.

Blaschke, L., Forstreuter, M., Sheppard, L. J., Leith, I. K., Murray, M. B., Polle, A. (2002). Lignification in beech (*Fagus sylvatica*) grown at elevated CO_2 concentrations: interaction with nutrient availability and leaf maturation. *Tree Physiology*, *22*(7), 469–477.

Cassan, O., Pimparé, L. L., Dubos, C., Gojon, A., Bach, L., Lèbre, S., Martin, A. (2023). A gene regulatory network in Arabidopsis roots reveals features and regulators of the plant response to elevated CO_2. *New Phytologist*, 239 (3), 992–1004.

Bahamonde, H. A., Aranda, I., Peri, P. L., Gyenge, J., Fernández, V. (2023). Leaf wettability, anatomy and ultra-structure of *Nothofagus antarctica* and *N. betuloides* grown under a CO_2 enriched atmosphere. *Plant Physiology and Biochemistry*, *194*, 193–201.

Du, Q. R., Lei, J. P., Liu, J. F., Wang, P. C., Xiao, W. F., Pan, L. (2014). Eco-physiological response of Quercus variabilis seedlings to increased atmospheric CO_2 and N supply. *Ying Yong Sheng tai xue bao. The Journal of Applied Ecology*, *25*(1), 24–30.

Ebi, K. L., Anderson, C. L., Hess, J. J., Kim, S. H., Loladze, I., Neumann, R. B., Singh, D., Ziska, L., Wood, R. (2021). Nutritional quality of crops in a high CO_2 world: An agenda for research and technology development. *Environmental Research Letters*, *16*(6), 064045. https://doi.org/10.1088/1748-9326/abfcfa.

Fernie, A. R., Roscher, A., Ratcliffe, R. G., Kruger, N. J. (2001). Fructose 2,6-bisphosphate activates pyrophosphate: fructose-6-phosphate 1-phosphotransferase and increases triose phosphate to hexose phosphate cycling in heterotrophic cells. *Planta*, *212*(2), 250–263. https://doi.org/10.1007/s004250000386.

Gao, L., Wang, W., Xu, C., Han, X., Li, Y., Liu, Y., Qi, H. (2022). Physiological and Transcriptomic Analyses Reveal the Effects of Elevated Root-Zone CO_2 on the Metabolism of Sugars and Starch in the Roots of Oriental Melon Seedlings. *International Journal of Molecular Sciences*, *23*(20), 12537.

Ghasemzadeh, A., Jaafar, H. Z. (2011). Effect of CO_2 enrichment on synthesis of some primary and secondary metabolites in ginger (*Zingiber officinale* Roscoe). *International Journal of Molecular Sciences*, *12*(2), 1101–1114.

Graaff, D M. A., Van Groenigen, K. J., Six, J., Hungate, B., v Kessel, C. (2006). Interactions between plant growth and soil nutrient cycling under elevated CO_2: a meta-analysis. *Global Change Biology*, *12*(11), 2077–2091.

Han, X., Sun, Y., Chen, J., Wang, Z., Qi, H., Liu, Y., Liu, Y. (2023). Effects of CO_2 Enrichment on Carbon Assimilation, Yield and Quality of Oriental Melon Cultivated in a Solar Greenhouse. *Horticulturae*, *9*(5), 561.

He, J., Qin, L., Lee, S. K. (2016). Root morphology, Plant growth, nitrate accumulation and nitrogen metabolism of temperate lettuce grown in the tropics with elevated root-zone CO_2 at different root-zone temperatures. *American Journal of Plant Sciences*, *7*(14), 1821–1833.

Hongxu, R., Xiong, C., Dongxiu, W. (2001). Effects of elevated CO_2 on photosynthesis and antioxidative ability of broad bean plants grown under drought condition. *Zuo wu xue bao*, *27*(6), 729–736.

Larios, B., Agüera, E., Cabello, P., Maldonado, J. M., Haba, D L P. (2004). The rate of CO_2 assimilation controls the expression and activity of glutamine synthetase through sugar formation in sunflower (*Helianthus annuus* L.) leaves. *Journal of Experimental Botany*, *55*(394), 69–75.

Luo, Z. B., Langenfeld-Heyser, R., Calfapietra, C., Polle, A. (2005). Influence of free air CO_2 enrichment (EUROFACE) and nitrogen fertilisation on the anatomy of juvenile wood of three poplar species after coppicing. *Trees*, *19*, 109–118.

Li, S., Li, Y., Gao, Y., He, X., Zhang, D., Liu, B., Li, Q. (2020). Effects of CO_2 enrichment on non-structural carbohydrate metabolism in leaves of cucumber seedlings under salt stress. *Scientia Horticulturae*, *265*, 109275.

Li, X., Zhang, G., Sun, B., et al. (2013). Stimulated Leaf Dark Respiration in Tomato in an Elevated Carbon Dioxide Atmosphere. *Scientific Reports 3*, 3433 (2013). https://doi.org/10.1038/srep03433.

Li, D., Dong, J., Gruda, N. S., Li, X., Duan, Z. (2022). Elevated root-zone temperature promotes the growth and alleviates the photosynthetic acclimation of cucumber plants exposed to elevated [CO_2]. *Environmental and Experimental Botany*, *194*, 104694.

Li, S., Li, Y., Gao, Y., He, X., Zhang, D., Liu, B., Li, Q. (2020). Effects of CO_2 enrichment on non-structural carbohydrate metabolism in leaves of cucumber seedlings under salt stress. *Scientia Horticulturae*, *265*, 109275.

Liu, J., Kang, S., Davies, W. J., Ding, R. (2020). Elevated [CO2] alleviates the impacts of water deficit on xylem anatomy and hydraulic properties of maize stems. *Plant, Cell & Environment*, *43*(3), 563–578.

Matimati, I., Verboom, G. A., Cramer, M. D. (2014). Nitrogen regulation of transpiration controls mass-flow acquisition of nutrients. *Journal of Experimental Botany*, *65*(1), 159–168.

Malamy, JE (2005) Intrinsic and environmental factors regulating root system growth. *Plant Cell & Environment*, *28*, 67–77.

Malamy, J.E (2010). Intrinsic and environmental response pathways that regulate root system architecture. *Plant Cell & Environment, 28*, 67–77.

Mir, S. A., Mukherjee, S., Makar, S., Pal, G. (2019). Cucurbitacins a vibrant triterpenoid: A review on its anticancer property. *PharmaTutor*, *7*(2), 43–54.

Nafziger, E. D., Koller, H. R. (1976). Influence of leaf starch concentration on CO_2 assimilation in soybean. *Plant Physiology*, *57*(4), 560–563.

Niinemets, Ü., Flexas, J., Penuelas, J. (2011). Evergreens favored by higher responsiveness to increased CO_2. *Trends in Ecology and Evolution*, *26*(3), 136-142.

Nunes-Nesi, A., Carrari, F., Gibon, Y., Sulpice, R., Lytovchenko, A., Fisahn, J., Graham, J., Ratcliffe, R. G., Sweetlove, L. J., Fernie, A. R. (2007). Deficiency of mitochondrial fumarase activity in tomato plants impairs photosynthesis via an effect on stomatal function. *Plant Journal*, *50*(6), 1093–1106. https://doi.org/10.1111/j.1365- 313X.2007. 03115.x

Porra, R.J., Thompson, W., Kriedemann, P. (1989). Determination of accurate extinction coefficients and simultaneous equations for assaying chlorophylls *a* and *b* extracted with four different solvents: verification of the concentration of chlorophyll standards by atomic absorption spectroscopy. *Biochimica et Biophysica Acta*, *975*, 384–394.

Pritchard, S. G., Rogers, H. H., Prior, S. A., Peterson, C. M. (1999). Elevated CO_2 and plant structure: a review. *Global Change Biology*, *5*(7), 807–837.

Pritchard, S. G., Ju, Z., van Santen, E., Qiu, J., Weaver, D. B., Prior, S. A., Rogers, H. H. (2000). The influence of elevated CO_2 on the activities of antioxidative enzymes in two soybean genotypes. *Functional Plant Biology*, *27*(11), 1061–1068.

Reddy, K. R., Robana, R. R., Hodges, H. F., Liu, X. J., McKinion, J. M. (1998). Interactions of CO_2 enrichment and temperature on cotton growth and leaf characteristics. *Environmental and Experimental Botany*, *39*(2), 117–129.

Salihi, M. S., Ahmad-Hamdani, M. S., Jusoh, M. (2023). The impact of carbon dioxide (CO_2) enrichment on rice (*Oryza sativa* L.) production: a review. *Pakistan Journal of Botany*, 55(3), 1197–1204.

Saha, Sauravi., Sehgal, V. K., Chakraborty, D. Pal, M. (2013). Growth behavior of kabuli chickpea under elevated atmospheric CO_2. *Journal of Agricultural Physics*, *13*(1), 55–61.

Sharma, H. C., War, A. R., Pathania, M., Sharma, S. P., Akbar, S. M., Munghate, R. S. (2016). Elevated CO_2 influences host plant defense response in chickpea against *Helicoverpa armigera*. *Arthropod-Plant Interactions*, *10*, 171–181.

Soares, J. C., Santos, C. S., Carvalho, S. M. P., Pintado, M. M., Vasconcelos, M. W. (2019). Preserving the nutritional quality of crop plants under a changing climate: importance and strategies. *Plant and Soil*, *443*(1–2), 1–26. https://doi.org/10.1007/s11104-019- 04229-0

Song, H., Li, Y., Xu, X., Zhang, J., Zheng, S., Hou, L., Li, M. (2020). Analysis of genes related to chlorophyll metabolism under elevated CO_2 in cucumber (*Cucumis sativus* L.). *Scientia Horticulturae*, *261*, 108988.

Takatani, N., Ito, T., Kiba, T., Mori, M., Miyamoto, T., Maeda, S. I., Omata, T. (2014). Effects of high CO_2 on growth and metabolism of *Arabidopsis* seedlings during growth with a constantly limited supply of nitrogen. *Plant & Cell Physiology*, *55*(2), 281–292.

Yu, J., Tang, X. X., Zhang, P. Y., Tian, J. Y., Cai, H. J. (2004). Effects of CO_2 Enrichment on Photosynthesis, Lipid peroxidation and activities of antioxidative enzymes of *Platymonas subcordiformis* subjected to UV-B radiation stress. *Acta Botanica Sinica*, *46*(6), 682–690.

Yu, J., Li, R., Fan, N., Yang, Z., Huang, B. (2017). Metabolic pathways involved in carbon dioxide enhanced heat tolerance in bermudagrass. *Frontiers in Plant Science*, 8, 1506.

Zhang, C., Akhlaq, M., Yan, H., Ni, Y., Liang, S., Zhou, J., Li, J. (2023). Chlorophyll fluorescence parameter as a predictor of tomato growth and yield under CO_2 enrichment in protective cultivation. *Agricultural Water Management*, *284*, 108333.

Figures

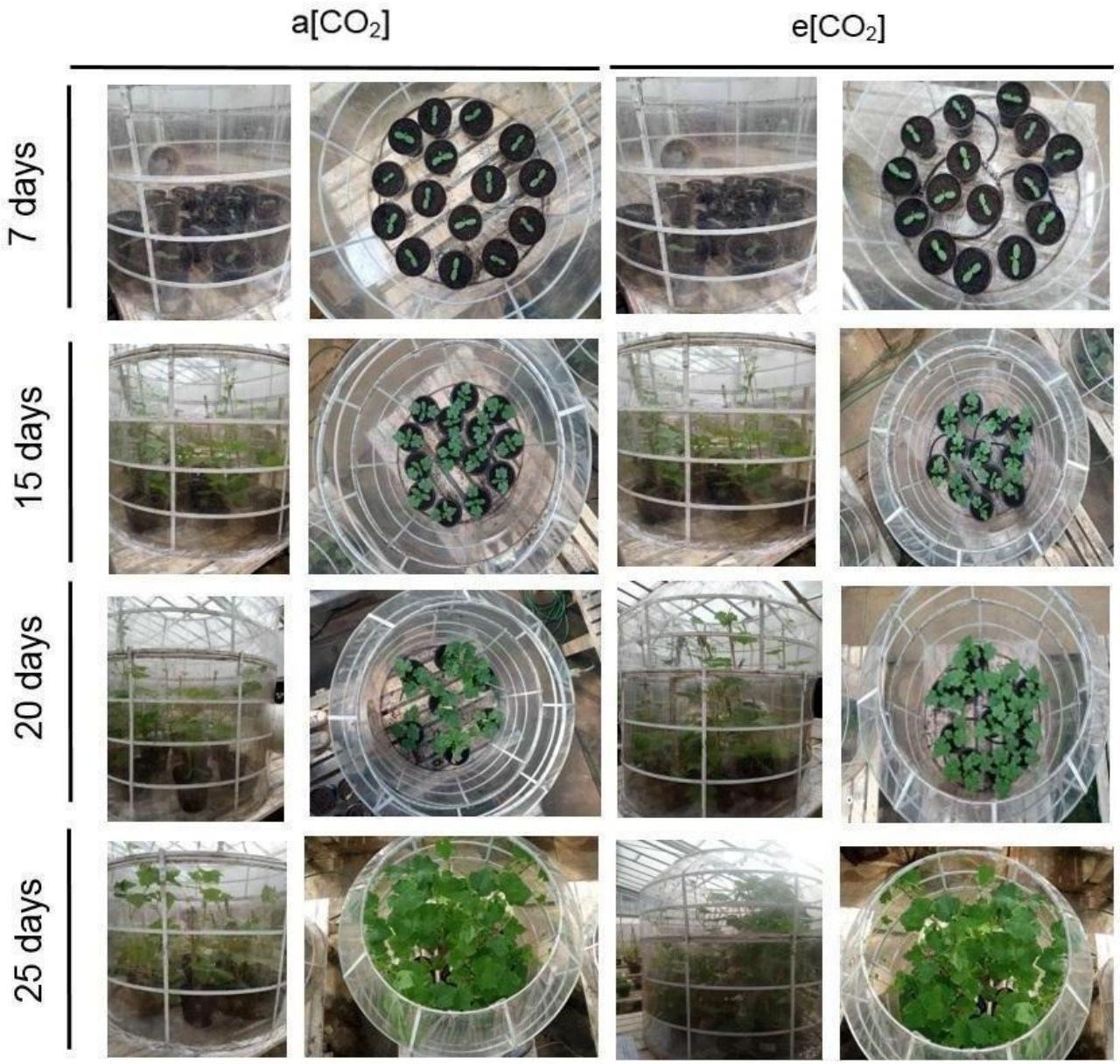

Figure 1. Overview of the CO_2-enriched experiment carried out with *Luffa cylindrica* at two CO_2 concentrations: ambient (a[CO_2]) (400ppm) and elevated (e[CO_2]) (800ppm) in open-top chambers under greenhouse conditions.

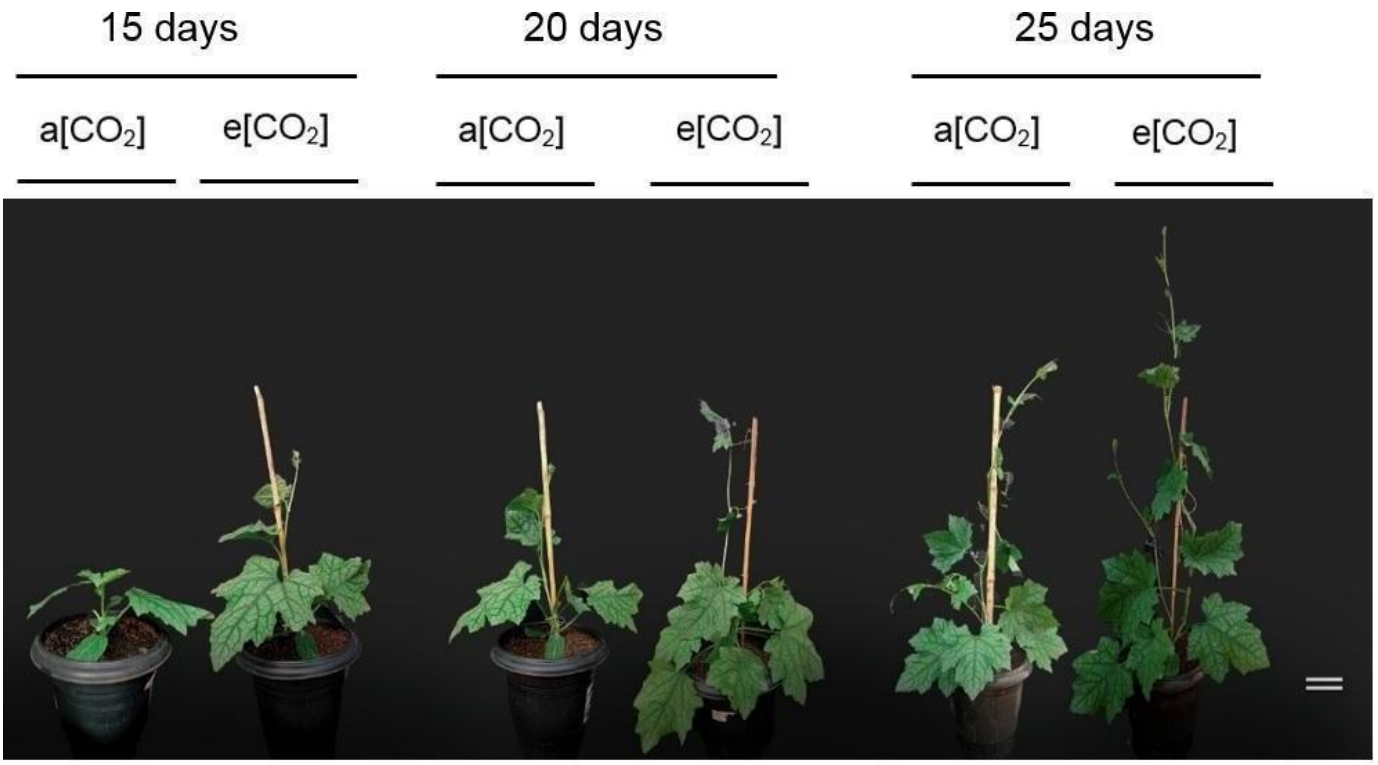

Figure 2. The visual aspect of *Luffa cylindrica* plants, grown for 15, 20, and 25 days, in open-top chambers, under ambient (a[CO_2]) and elevated (e[CO_2]) CO_2 concentration. Bar = 5 cm.

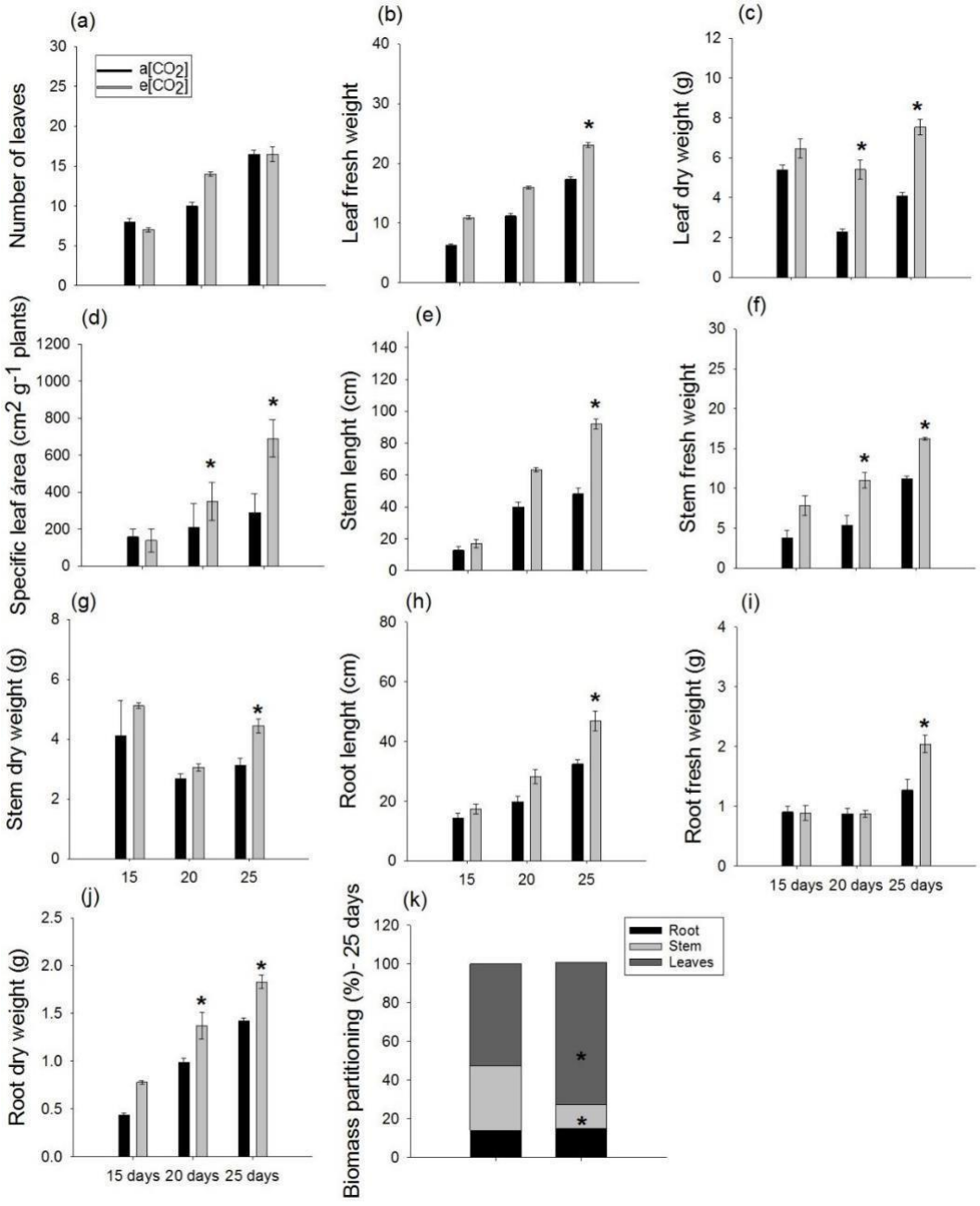

Figure 3. Variation of biometric parameters in *Luffa cylindrica* L. plants grown for 15, 20, and 25 days under ambient (a[CO_2]) and elevated (e[CO_2]) CO_2 concentration. (**a**) Number of leaves; (**b**) Leaf fresh weight; (**c**) Leaf dry weight; (**d**) Specific leaf area; (**e**) Stem height; (f) Stem fresh weight; (**g**) Stem dry weight; (**h**) Root height; (**i**) Root fresh weight; (**j**) Root

dry weight; (**k**) Biomass composition.Values presented as means (n = 5) ± standard error. Asterisks indicate a significant difference (ANOVA; $P \leq 0.05$).

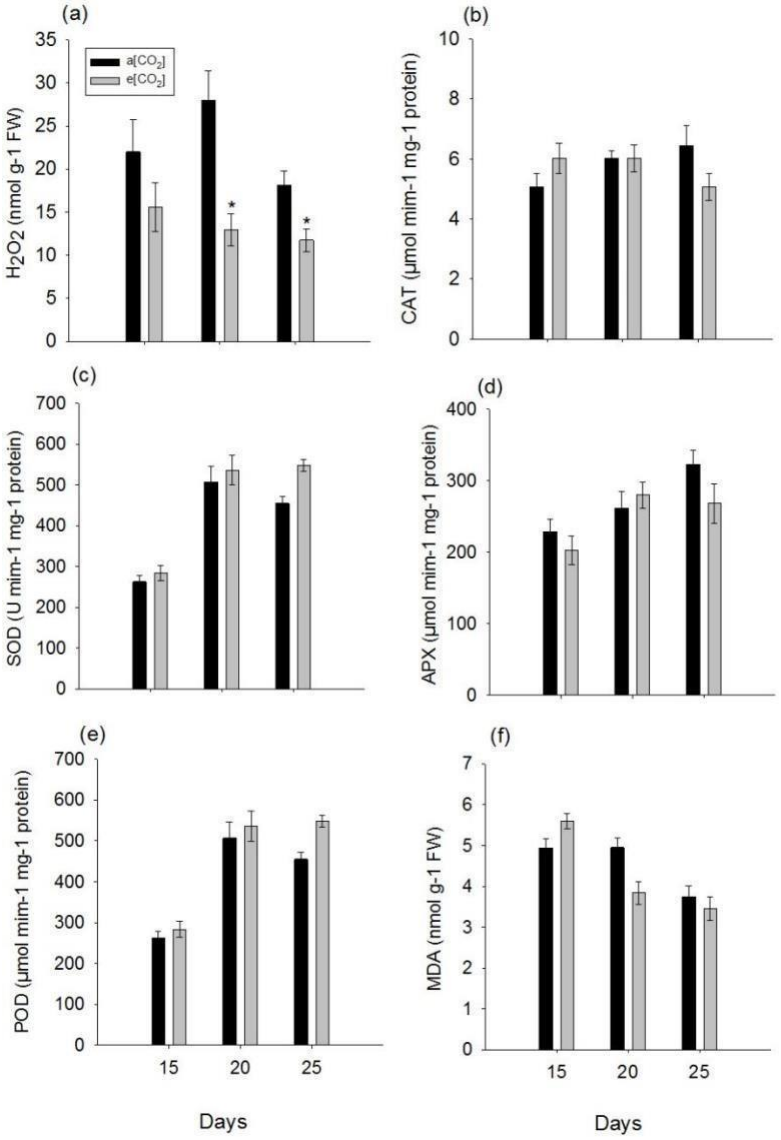

Figure 4. Activity of enzymes involved in antioxidation and malonaldehyde (MDA) content in leaves of *Luffa cylindrica* plants grown for 15, 20 and 15 days under ambient (a[CO_2]) and elevated (e[CO_2]) CO_2 concentration. (**a**) Catalase (CAT); (**b**) Free peroxides (H2O2); (c) superoxide dismutase (SOD); (d) ascorbate peroxidase (APX); (e) peroxidases (POD); (f) malonaldehyde (MDA). Values are presented as means (n=5) ± standard error (ANOVA; $P \leq 0.05$).

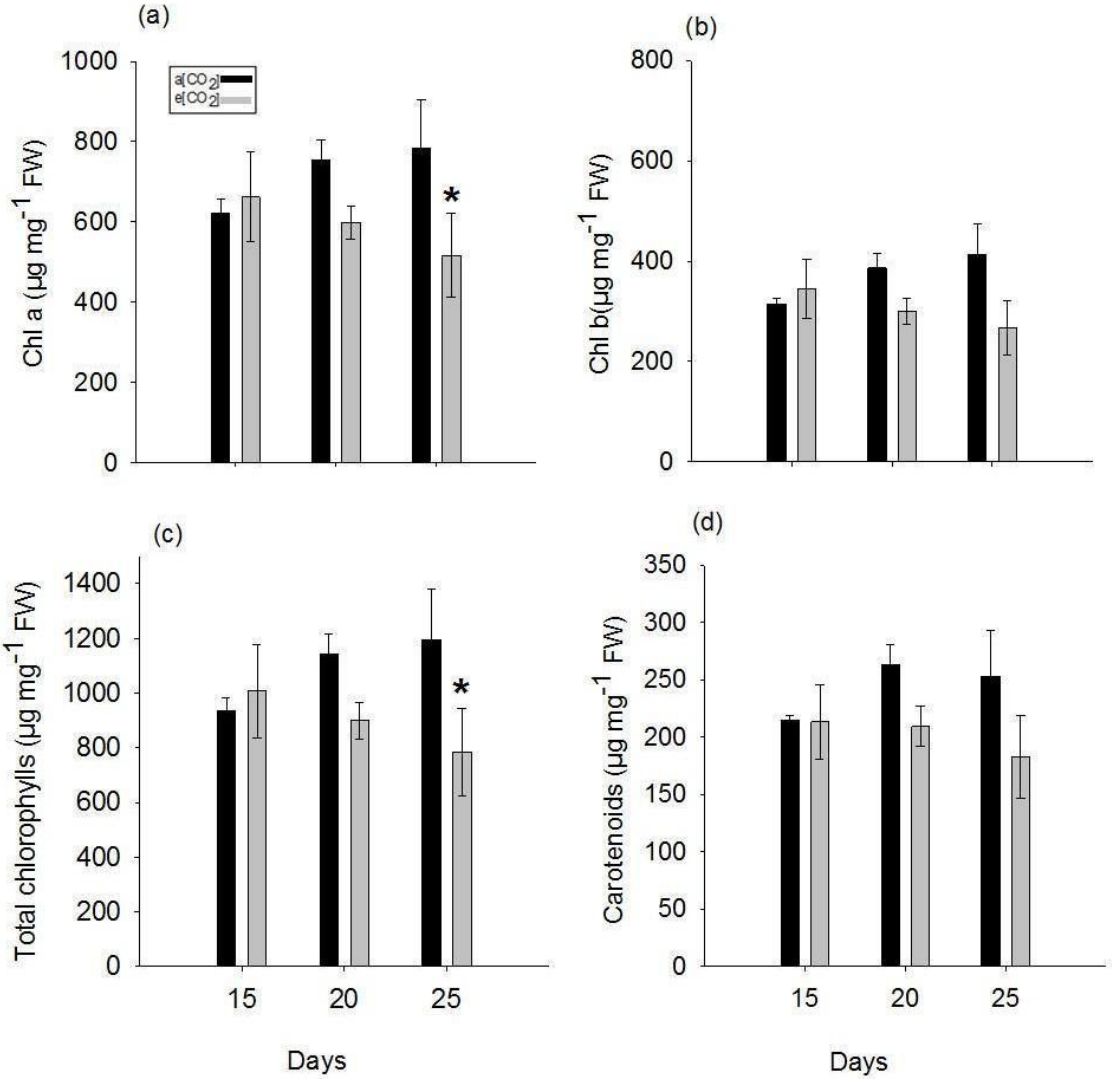

Figure 5. Pigment content in leaves of *Luffa cylindrica* plants grown for 15, 20 and 25 days under ambient (a[CO_2]) and elevated (e[CO_2]) CO_2 concentrations. (**a**) Chlorophyll *a* (Chl*a*); (**b**) Chlorophyll *b* (Chl*b*); (**c**) Total chlorophyll; (**d**) Carotenoids. Values are

presented as means (n=5) ± standard error. Asterisks indicate a significant difference (ANOVA; $P \leq 0.05$).

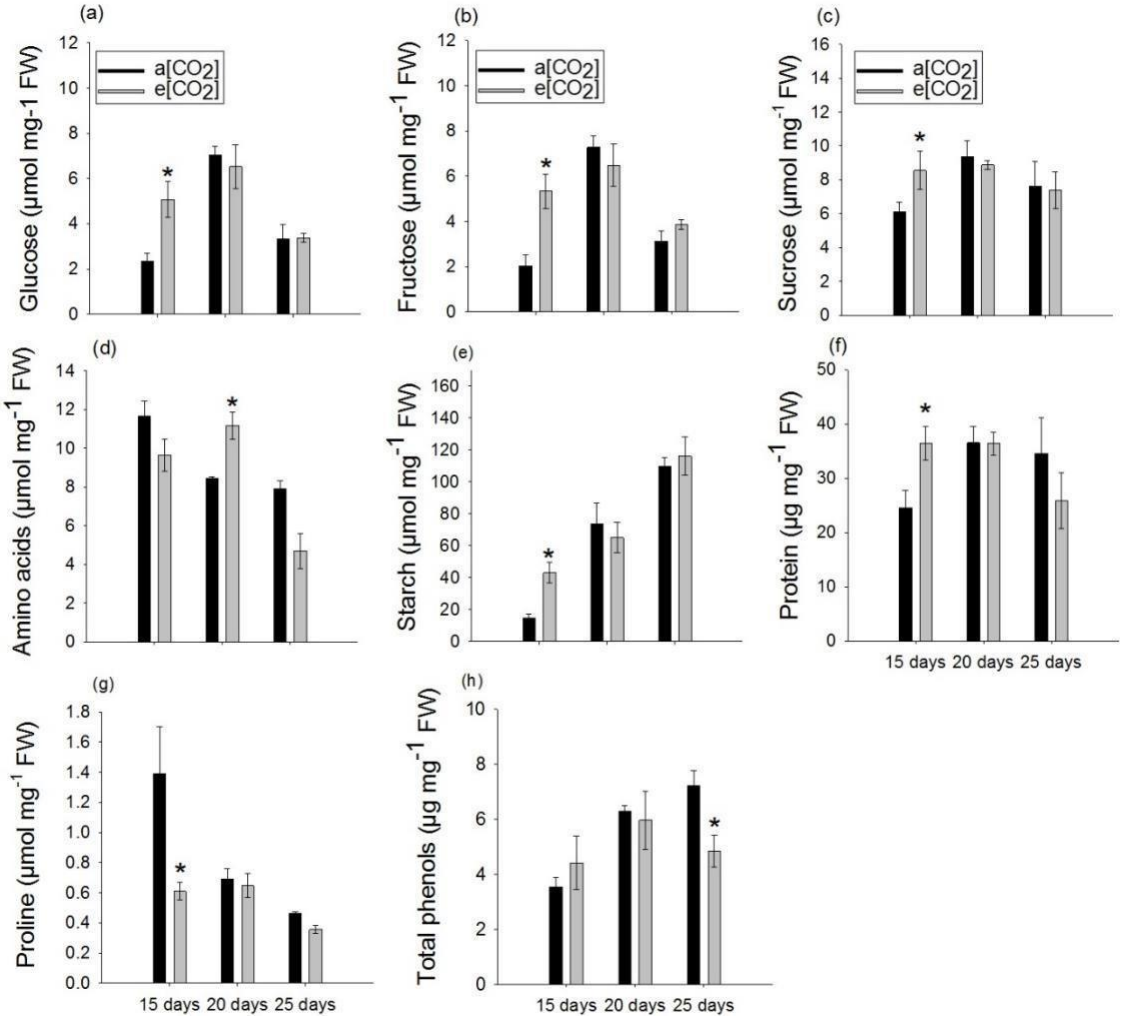

Figure 6. Changes in the content of metabolites involved in carbon metabolism in leaves of *Luffa cylindrica* plants grown for 15, 20, and 25 days under ambient (a[CO_2]) and elevated (e[CO_2]) CO_2 concentrations. (**a**) Glucose; (**b**) Fructose; (**c**) Sucrose; (**d**) Amino acids; (**e**) Starch; (**f**) Protein; (**g**) Proline and (**h**) Total phenols. Values are presented as

means (n=5) ± standard error. Asterisks indicate a significant difference (ANOVA; $P \leq 0.05$).

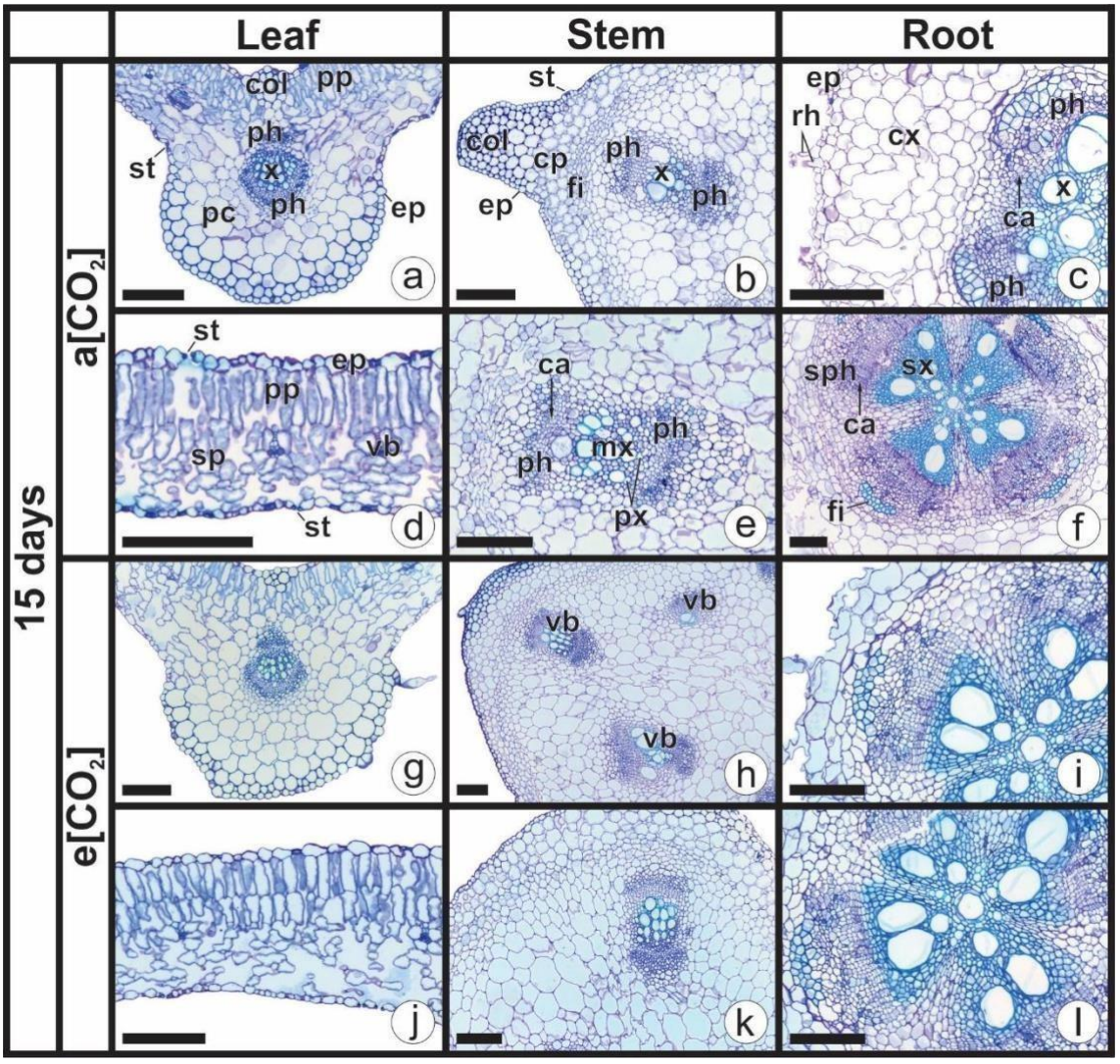

Figure 7. Cross-sections of the central vein of the leaf, stem and root of *Luffa cylindrica* plants grown for 15 days under ambient (a[CO_2]) and elevated (e[CO_2]) CO_2 concentrations. a- f (leaf, stem and root under ambient CO_2 conditions); G- g-l (leaf, root,

stem) under high CO_2 conditions. *Abbreviations: pp* = palisade parenchyma; col= collenchyma; *ph*= phloem; *st*= stomata; *pc*= parenchyma cells; *ep*= epidermal cells; *fi*= fibers; *cx*= cortex; *mx* = metaxylem; *px* = protoxylem; *ca*= cambium; *rh*= ray; *sph*= secondary phloem; *sx* = secondary xylem. Bars = 200 µm.

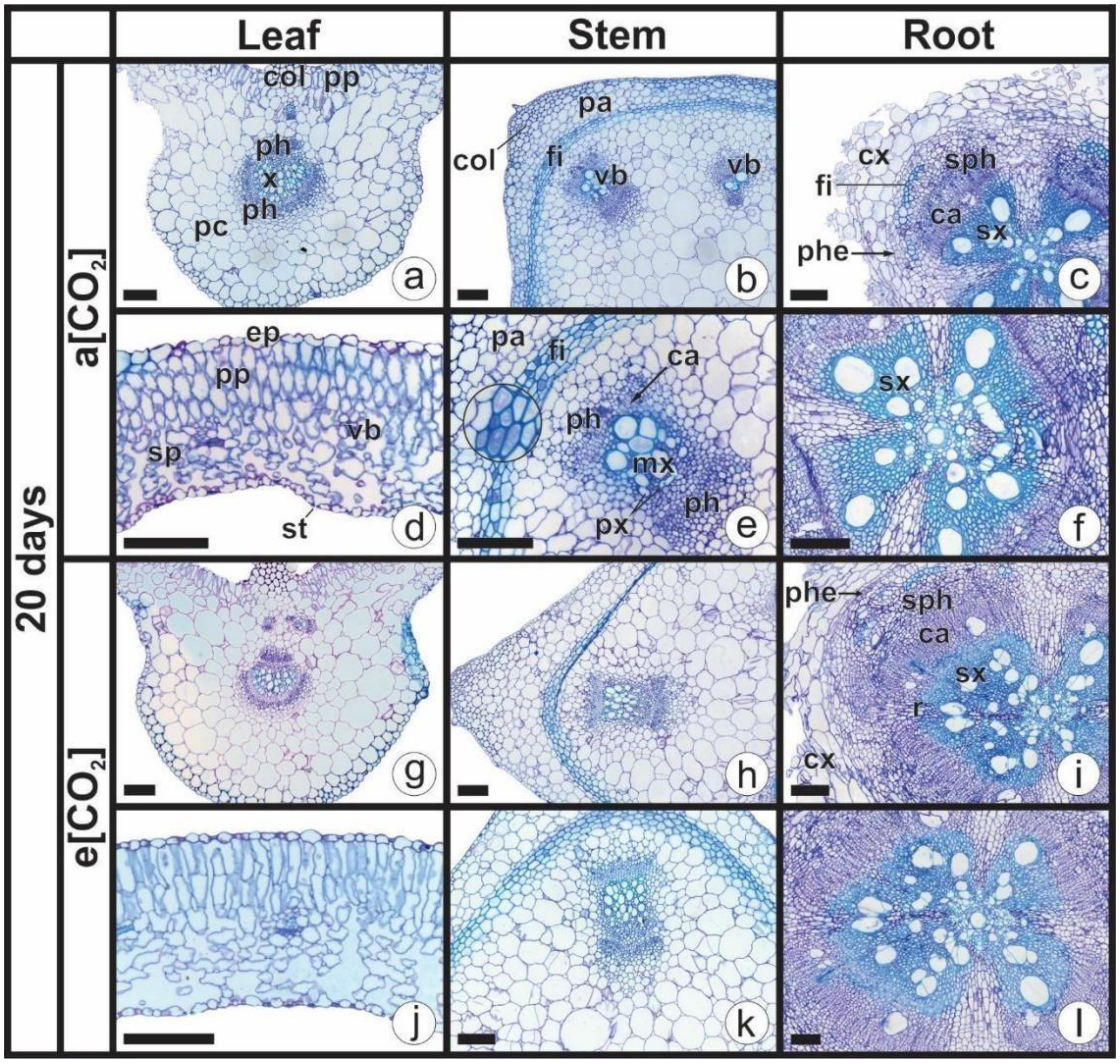

Figure 8. Cross-sections of the central vein of the leaf, stem and root of *Luffa cylindrica* plants grown for 20 days under ambient (a[CO_2]) and elevated (e[CO_2]) CO_2 concentrations. a-f (leaf, stem and root under ambient CO_2 conditions); g-l (leaf, root, stem) under high CO_2 conditions. *Abbreviations: pp* = palisade parenchyma; *col*= collenchyma; *ph*= phloem; st= stomata; *pc*= parenchyma cells; *ep*= epidermal cells; *fi*= fibers; *cx*= cortex; rh= ray; *ca*= cambium; *px*= protoxylem; *mx* = metaxylem; *sx*= secondary xylem; *sph* = secondary phloem; *vb* = vascular bundle. Bars = 200 µm.

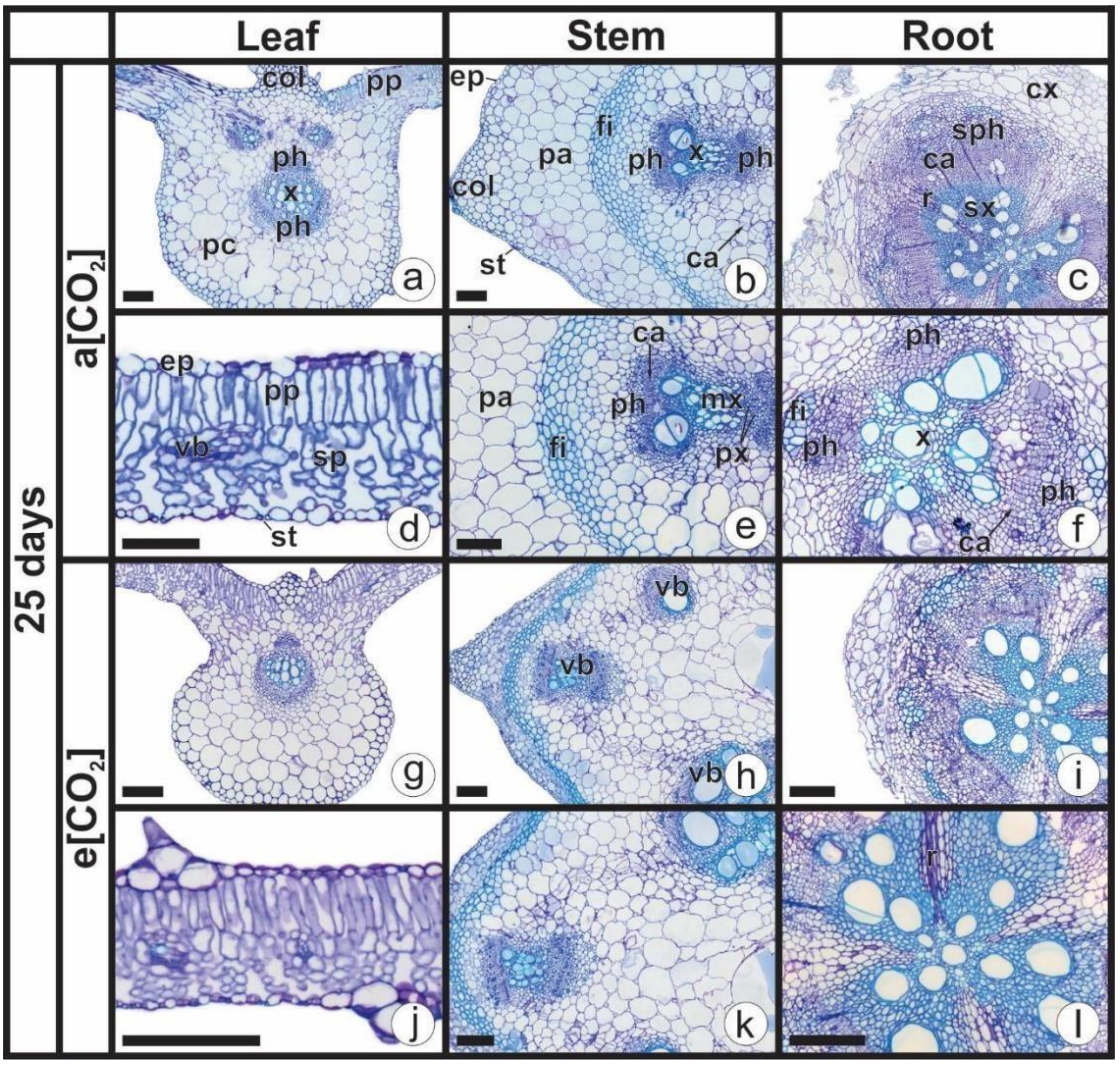

Figure 9. Cross-sections of the central vein of the leaf, stem, and root of *Luffa cylindrica* plants grown for 25 days under ambient (a[CO_2]) and elevated (e[CO_2]) CO_2 concentrations. a-f (leaf, stem, and root under ambient CO_2 conditions); g-l (leaf, root, stem) under high CO_2 conditions. *Abbreviations: pp* = palisade parenchyma; *col*= collenchyma; *ph*= phloem; *st*= stomata; *pc*= parenchyma cells; *ep*= epidermal cells; *fi*= fibers; *cx*= cortex; *rh*= ray; *ca*= cambium; *px*= protoxylem; *mx* = metaxylem; *sx*= secondary xylem; *sph* = secondary phloem; *vb* = vascular bundle. Bar= 200 µm.

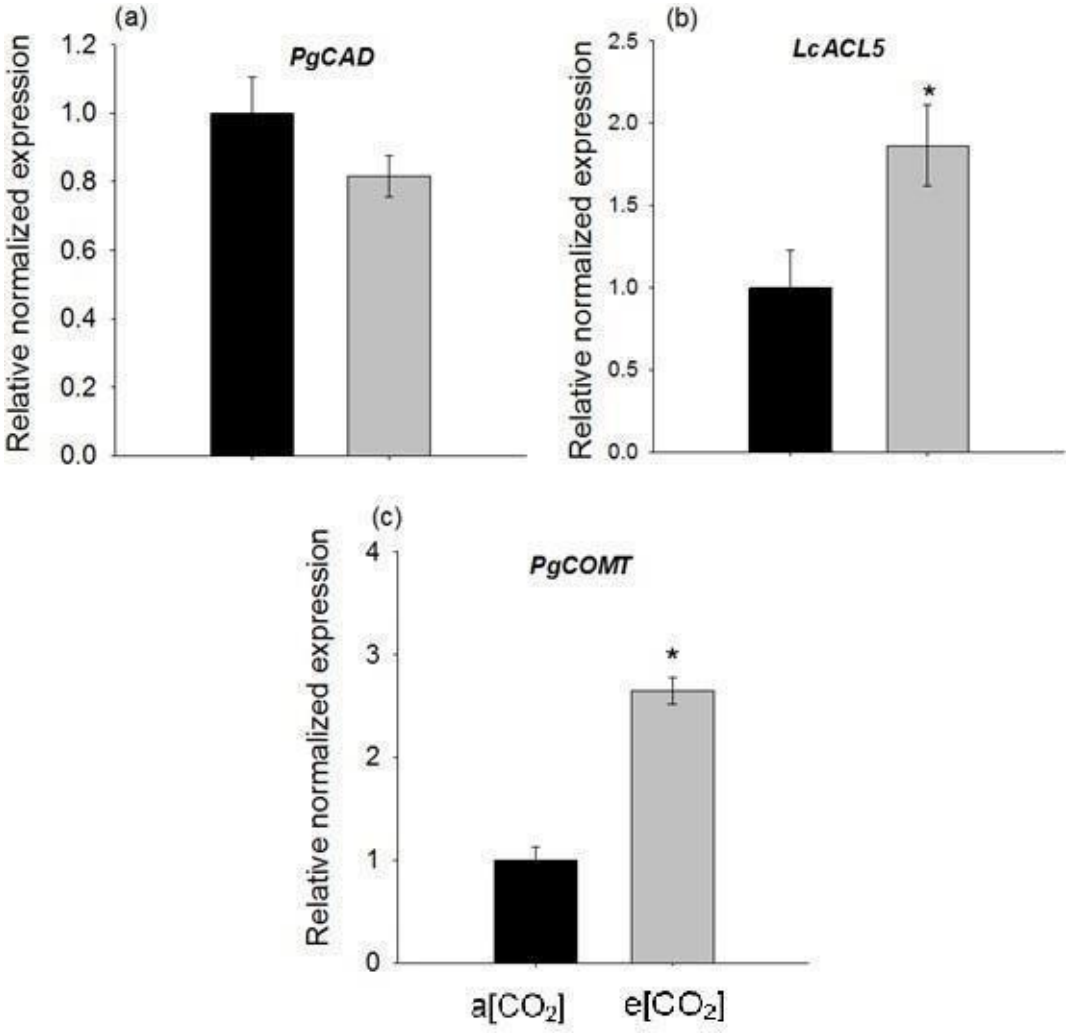

Figure 10. Relative expression of lignin and polyamine synthesis pathway genes in *Luffa cylindrica* plants grown for 25 days under ambient (a[CO_2]) and elevated (e[CO_2]) CO_2 concentrations. (**a**) *PgCAD*; (**b**) *LcACL5,* (**c**) *PgCOMT*. The RPS9 gene normalized

expression. Values are presented as means (n=3) ± standard error. Asterisks indicate significant difference (Dunnet; $P \leq 0.05$).

Suplementary material

Table 01: Primes and Sequences Used

Primer	Name	Sequence 5'-3'
LcACL5	*Thermospermine synthase*	AGCCTAGATTGAAACAAGATGGCA-**F** GGGCAGAATAAGGCACCACA- **R**
LcPAO	*Polyamine oxidase*	TGATTATTGGGGCGGGAATGG-**F** TCCGTCGTGTTGATTCTGCC- **R**
LcSPDE	*Spermidine synthase*	GACATTGTTACCAACTGCCGC-**F** ACCCAAGAGATGCCGATAAGC-**R**
PgCAD	*Cinnamyl alcohol dehydrogenase*	GATTCAACTGCGCCCCTCTT- **F** ACCAAGCCCTCCTAAACCAC-**R**
BoRPS9 (gene reference)	*Ribosomal protein S9*	ACTTCTCTCTCACCAGTCCGT- **F** GCCTTCTTCATGGAGGCCTT- **R**
PgCOMT	*Caffeic acid 3-O-methyltransferase*	TTCGCATTTGTTGAGGCTGA- **F** AGGAAACGCGACAGAACCAA- **R**

General conclusions

Under the experimental conditions, the obtained data led us to the following conclusions:

Under the experimental conditions, the obtained data led us to the following conclusions:

- PBZ can influence the differentiation of TEs, reorganizing metabolism and activating essential pathways for plant growth;

- PBZ alters plant size at all the concentrations studied;

- High CO_2 conditions promote the growth and development of *Luffa Cylindrica*

- It can be considered that the *Luffa cylindrica* species has such defined mechanisms that allow it to survive the different conditions imposed.

These findings are crucial for understanding the molecular and biochemical mechanisms underlying these events, providing valuable insights for refining breeding strategies, improving plant yields and addressing environmental challenges.